Evaporation from the Earth' Surface

Jürgen Grieser

May 3, 2011

Contents

Chapter 1

Actual, Potential and Grass-Reference Evapotranspiration

In this manuscript evaporation is the flux of water from the earth' surface into the atmosphere. It is the amount of water that gets lost from the surface per time interval and area and thus has units of mass per time per area. According to SI units this is expressed as $kg/s/m^2$. However, meteorologists prefer to use the same units as for the reverse flow, precipitation, which most frequently is provided in mm/day. The transformation is very direct since $1kg$ of water spread over $1m^2$ of surface has a depth of $1mm$ and thus, $1kg/m^2$ water equals $1mm$ water depth, given the density of water as $1000kg/m^3$.

Knowing the latent heat of evaporation $L = 2.45 \times 10^6 \frac{J}{kg}$ we can express evaporation also by the energy E that is needed to evaporate the water. This is particularly handy if energy flux densities are expressed in $MJ/m^2/day$ since in this case $1MJ/m^2/day$ equals $\frac{1}{2.45}mm/day = 0.408mm/day$. Note that L is a function of temperature which is shortly discussed in appendix A.

If totally covered with water, the surface has no influence on evaporation. In this case the evaporation is called **potential evaporation**. However, other than water surfaces can lack of water availability. This causes the actual evaporation to be below the potential evaporation. The mechanism that decreases the actual vs. the potential evaporation is sometimes described by a soil resistance. On the other hand, evaporation can be enhanced due to plants. They add additional surface (the leaves) and can effectively "pump" soil water to this surface. The leaf area index LAI is the ratio of green plant surface to ground surface and is often used as an indicator of the importance of a vegetation cover. The process of evaporation via plants is called transpiration. The total evaporation from an area with vegetation is therefore determined by both transpiration and evaporation. This is the reason why evaporation from a surface covered with plants is usually called **evapotranspiration**. The actual evapotranspiration of a vegetated surface can be considerably larger than the evaporation from a water surface just due to a large LAI and the "pumping" of soil water by the plant.

In order to model the evaporation for different plants as well as for inter-comparison

of different regions a standard vegetation is introduced which has well defined features. This standard is a grass with $h = 12cm$ depth, an albedo of $\alpha = 0.23$ and an LAI of 2.88 according to FAO. The evaporation from this reference surface is called **grass reference evapotranspiration** ETo. Crop coefficients k_c are the ratio of the maximum possible (i.e. not limited by water shortage) evapotranspiration of the respective crops in their current state of development to ETo. The knowledge of crop coefficients therefore allows for the calculation of the water demand of crops and - in case that enough water is available - the actual evapotranspiration if ETo is known.

Several indices are derived in order to hydrologically characterize local and regional climates. Two examples are the Climatic Moisture Index (CMI) which is the ratio of rainfall to potential evapotranspiration and the soil moisture index (SMI) which is the ratio of actual evapotranspiration to potential evapotranspiration.

Chapter 2

Estimation of Evaporation using the Energy Balance

2.1 The Energy Balance of a Surface

The energy balance of a surface in equilibrium with its surrounding is

$$0 = Q_0 - G_0 - H_0 - E_0 \tag{2.1}$$

where

$$\begin{array}{rcl} Q_0 & = & \text{radiation balance of the surface,} \\ G_0 & = & \text{heat transfer into the ground,} \\ H_0 & = & \text{sensible heat flux into the atmosphere,} \\ E_0 & = & \text{latent heat flux into the atmosphere} \end{array}$$

where the index 0 stands for zero height, i.e. the surface. Q_0 is positive if the surface gains energy from the radiation balance. H_0 and E_0 are counted positive if the fluxes are in positive z direction (away from the surface) while the heat flux into the ground is positive in negative z direction (again away from the surface).

The next section describes the evaporation as a result of the energy balance of a wet surface.

2.2 Difference Method and Potential Evaporation

The difference method (or bulk method) is an easy way to approximate fluxes by the difference of a potential and a transport coefficient. We apply it to the sensible and latent heat flux and write

$$\begin{array}{rcl} H_0 & = & -\alpha_H(\theta_2 - \theta_0) \approx -\alpha_H(T_2 - T_0) \\ E_0 & = & -\alpha_W(q_2 - q_0) \end{array} \tag{2.2}$$

where the index 2 stands for two meters above surface. θ means the potential temperature. The potential temperature difference between zero and two meters can nicely be approximated by the temperature difference of these heights. q stands for the specific

humidity observed in kg water vapor per kg air. Finally α_H and α_W are the transport coefficients of energy due to heat and water transfer between the surface and $2m$ above the surface, respectively. The transport coefficients are linked by

$$\alpha_W = \alpha_H \frac{L}{c_p} \tag{2.3}$$

with the latent heat of evaporation L and the heat capacity of air at constant pressure $c_p = 1004 J/kg/K$. The units of α_H and α_W are $\frac{J}{m^2 K s}$ and $\frac{J}{m^2 s}$, respectively. In order to estimate E_0 we therefore need to know q_0, q_2 and α_H. q_2 is a meteorological observable, available for many locations on Earth. q_0, however, has to be estimated. To do so, we make the assumption that evaporation from the surface is not limited by any water supply from the surface. In this case the specific humidity at the surface, q_0, equals the saturation specific humidity q_{0s} at the surface, where the index s stands for saturation.

Specific humidity q is uniquely linked to water vapor pressure e by the ratio $\varepsilon = 0.622$ of molecular mass of water to dry air and the air pressure p as

$$q = \varepsilon \frac{e}{p}. \tag{2.4}$$

Taking that into account and using eq. (2.3) we get

$$E_0 = \alpha_W (q_0 - q_2) = \frac{\alpha_H}{\gamma} (e_{0s} - e_2) \tag{2.5}$$

with the psychrometric constant

$$\gamma = \frac{p\, c_p}{\varepsilon\, L}. \tag{2.6}$$

We approximate $e_{0s} = e_s(T_0)$ by linearization as

$$e_{0s} \approx e_{2s} + \left.\frac{\partial e_s}{\partial T}\right|_{T_2} (T_0 - T_2) \tag{2.7}$$

and name $\left.\frac{\partial e_s}{\partial T}\right|_{T_2} = \Delta$. This leads to

$$E_0 = \frac{\alpha_H}{\gamma} \left[\Delta (T_0 - T_2) + e_{2s} - e_2\right]. \tag{2.8}$$

The latter term on the rhs can be reformulated with the relative humidity f as

$$e_{2s} - e_2 = e_{2s} - f \cdot e_{2s} = e_{2s}(1 - f) \tag{2.9}$$

yielding

$$E_0 = \frac{\alpha_H}{\gamma} \left[\Delta (T_0 - T_2) + e_{2s}(1 - f)\right]. \tag{2.10}$$

From eq. (2.1) and (2.2) we also know that

$$H_0 = \alpha_H (T_0 - T_2) = Q_0 - G_0 - E_0 \tag{2.11}$$

which we use to replace $(T_0 - T_2)$ in eq. (2.10) to get

$$\gamma E_0 = \Delta (Q_0 - G_0) - \Delta E_0 + \alpha_H e_{2s}(1 - f) \tag{2.12}$$

Reordering eq. (2.12) yields

$$E_0 = \frac{\Delta(Q_0 - G_0) + \alpha_H e_{2s}(1-f)}{\gamma + \Delta} \tag{2.13}$$

which is the energy flux due to **potential evaporation**.

E_0 is the sum of two terms

$$\begin{aligned} E_{0,Rad} &= \frac{\Delta(Q_0 - G_0)}{\Delta+\gamma} \\ E_{0,Vent} &= \frac{\alpha_H\, e_{2s}\,(1-f)}{\Delta+\gamma}. \end{aligned} \tag{2.14}$$

of which the first is usually called radiation term while the second is named ventilation term. We see that only the latter depends on humidity. The higher the humidity the lower the ventilation term. The term vanishes in case of hundred percent relative humidity. In this case evaporation is driven solely by radiation and ground-heat flux. Note that even 100% relative humidity at both, surface and $2m$ height does not mean that there is no evaporation from the surface. A positive radiation balance at the surface may warm the surface with respect to $2m$ height leading to higher q_{0s} than q_{2s}.

Before we look into estimations of α_H and the case of surface resistance, we derive an equation for the surface temperature T_0 in the following section.

2.3 Surface Temperature in case of Potential Evaporation

We can reorder eq. (2.11) to get an expression for the surface temperature as

$$T_0 = T_2 + \frac{Q_0 - G_0}{\alpha_H} - \frac{E_0}{\alpha_H} \tag{2.15}$$

and insert eq. (2.13) for E_0 to get

$$\begin{aligned} T_0 &= T_2 + \left(\tfrac{1}{\alpha_H} - \tfrac{\Delta}{(\Delta+\gamma)\alpha_H}\right)(Q_0 - G_0) - \tfrac{e_{2s}}{\Delta+\gamma}(1-f) \\ &= T_2 + \tfrac{1}{\alpha_H}\left(\tfrac{\gamma}{\Delta+\gamma}\right)(Q_0 - G_0) - \tfrac{e_{2s}}{\Delta+\gamma}(1-f). \end{aligned} \tag{2.16}$$

The second term on the rhs describes the heating of the surface due to the radiation balance and the ground heat flux while the third term describes the cooling of the surface due to evaporation. Note that $T_2 - T_0$ is largest in case of $f = 1$ which minimizes evaporation.

Chapter 3

Potential Evaporation and Bowen Ratio

3.1 Bowen Ratio

The Bowen ratio is the ratio of sensible to latent heat flux from the surface and therefore given by

$$\beta = \frac{H_0}{E_0} = \frac{\gamma(T_0 - T_2)}{e_0 - e_2}. \tag{3.1}$$

For potential evaporation we got

$$e_0 - e_2 = e_{0s} - e_2 = \Delta(T_0 - T_2) + e_{2s}(1 - f) \tag{3.2}$$

and thus for the Bowen ratio in case of potential evaporation β_p

$$\beta_p = \frac{\gamma(T_0 - T_2)}{\Delta(T_0 - T_2) + e_{2s}(1 - f)}. \tag{3.3}$$

We see that the larger the relative humidity the larger the Bowen ratio. In case of water saturation in two meters height ($f = 1$) we get

$$\beta_p(f = 1) = \frac{\gamma}{\Delta}. \tag{3.4}$$

Therefore, eq. (3.4) provides the ratio of sensible to latent heat flux from a wet surface if the latent heat flux is minimized due to highest possible humidity. In this case it is independent of the temperature difference between the surface and $2m$ height.

γ depends on pressure p which decreases with elevation, while Δ depends on temperature T which usually also decreases with elevation. In the next section we analyze these relations and estimate the influence of elevation on the Bowen ratio.

3.2 Estimation of γ and Δ

According to eq. (2.6) the psychrometric constant γ is a function of the air pressure p. The latter can be estimated from an isentropic atmosphere as

$$p(z) = p_0 \left(\frac{T_0 + \frac{\partial T}{\partial z} \cdot z}{T_0} \right)^{\frac{-g}{R \frac{\partial T}{\partial z}}} \tag{3.5}$$

with

$$\begin{array}{rcl} p_0 & = & \text{surface pressure at } z = 0, \\ T_0 & = & \text{2m air temperature at } z = 0, \\ \frac{\partial T}{\partial z} & = & \text{vertical temperature gradient}, \\ g & = & \text{earth acceleration} = 9.81 m/s^2, \\ R & = & \text{gas constant of dry air} = 287 \frac{J}{K\,kg}, \textit{and} \\ c_p & = & \text{heat capacity of dry air at constant pressure} = 1004 kJ/K/kg. \end{array} \tag{3.6}$$

For a standard atmosphere one can assume $T_0 = 293K$, $p_0 = 1013hPa$, and $\frac{\partial T}{\partial z} = -0.0065K/m$. Using these values eq. (3.5) reduces to

$$p \approx 1013 \left(\frac{293 - 0.0065z}{293} \right)^{5.26}. \tag{3.7}$$

Using further $\varepsilon = 0.622$, $L = 2.45MJ/kg$, and $c_p = 1004J/kg/K$ we get

$$\gamma = \frac{.658 \times 10^{-3}}{K} p. \tag{3.8}$$

Fig. 3.1 shows the decrease of γ with altitude for a standard atmosphere. The dependence on T_0 becomes more relevant for larger elevations and can reach 10% in $5000m$. Usually this dependence is neglected and $T_0 = 20°C$ is used. Relative variations in air pressure due to weather variability are of the order of $\frac{10hPa}{1000hPa}$ and therefore do not exceed a couple of percents.

$\Delta = \frac{de_s}{dT}$ is the slope of the saturation vapor pressure $e_s(T)$. The latter function is a solution of the Clausius-Clapeyron equation. A common approximation is the Magnus formula

$$e_s(T_C) = 6.108hPa \exp \left(\frac{17.27\,T_C}{T_C + 237.3°C} \right) \tag{3.9}$$

with the temperature T_C in $°C$.

After a bit of calculus we get

$$\Delta(T_C) = \frac{de_s}{dT_C} = 6.108hPa \frac{17.27 \cdot 237.3°C}{(T_C + 237.3°C)^2} \exp \left(\frac{17.27 T_C}{T_C + 237.3°C} \right) \tag{3.10}$$

and in the case that temperature is given in K

$$\Delta(T_K) = \frac{de_s}{dT} = \frac{6.108hPa\,17.27 \cdot 237.3K}{(T_K - 35.85K)^2} \exp \left(\frac{17.27(T_K - 273.15K)}{T_K - 35.85K} \right). \tag{3.11}$$

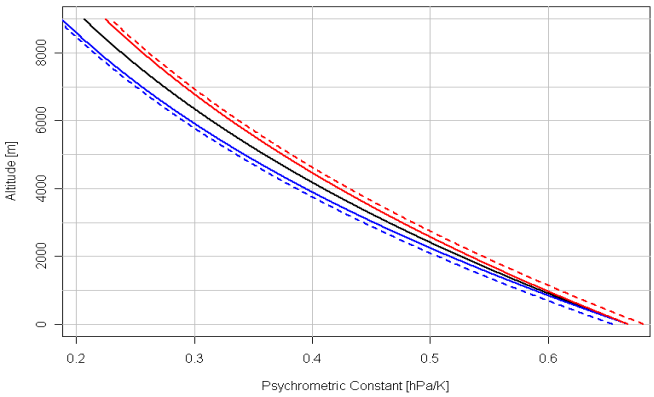

Figure 3.1: Psychrometric constant γ as function of elevation in case of $T_0 = 0°C$ (blue line), $T_0 = 20°C$ (black line), and $T_0 = 40°C$ (red line) for $p_0 = 1013.15hPa$ as well as for $T_0 = 0°C$ and $p_0 = 983hPa$ (blue dashed line) and for $T_0 = 40°C$ and $p_0 = 1033.15hPa$ (red dashed line).

Δ depends strongly on T and the dependency increases with increasing temperature as can be seen from Fig. 3.2. According to eq. (2.13) higher values of Δ mean higher weight for the radiation term of evaporation. Generally, temperature decreases with elevation which means that higher locations are expected to have lower values of Δ. If we assume $T_0 = 20°C$ and a vertical lapse rate of $-.65k/100m$ we get the strong decrease of Δ with height as shown in Fig. 3.3.

Both, γ and Δ decrease with elevation. Under standard conditions of $p_0 = 1013.15hPa$, $T_0 = 20°C$ and a vertical lapse rate of $-.65k/100m$ we get $\gamma(z = 0) = .6675hPa/K$ and $\Delta(z = 0) = 1.4475hPa/K$. For an elevation of $2000m$ we get$\gamma(z = 2000m) = .5258hPa/K$ and $\Delta(z = 2000m) = .6879hPa/K$. This is a reduction of about 52.5% in Δ but only 21% in γ. It shows that with higher elevation the ventilation term becomes more important even if neither wind speed nor specific humidity change.

Fig. 3.4 shows a map of the psychrometric constant for the locations in the FAO agromet database. There is no seasonal dependency since surface pressure is assumed to show no annual cycle. According to figures 3.5 and 3.6 Δ varies considerably with the annual cycle. This has an impact on the annual cycle of the evaporation and Bowen ratio.

3.3 Maximum Potential Bowen Ratio as a Function of Elevation

According to eq. (3.4) the maximum potential Bowen ratio is

$$\beta_p(f = 1) = \frac{\gamma}{\Delta}. \tag{3.12}$$

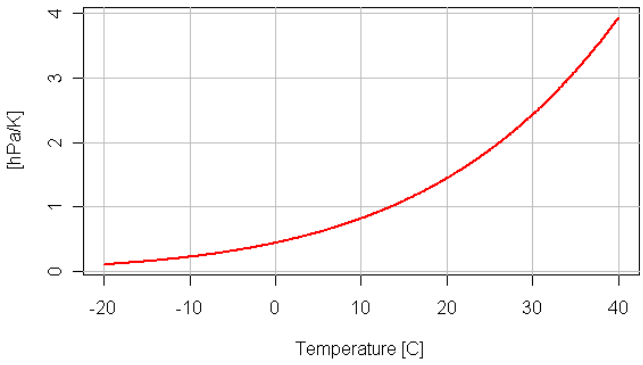

Figure 3.2: Slope $\Delta = \frac{de_s}{dT}$ of the saturation water vapor dependency on temperature.

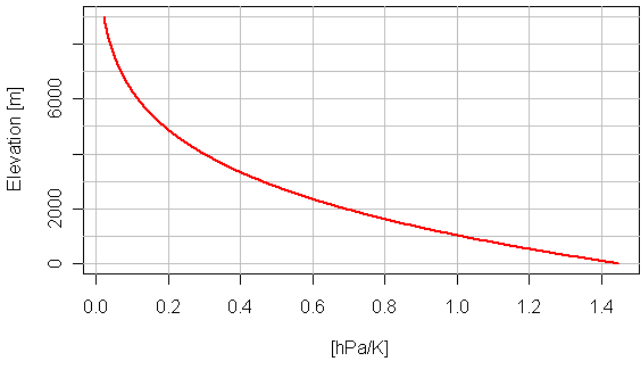

Figure 3.3: Slope of the saturation water vapor dependency on temperature as function of elevation for $T_0 = 293K$ and a lapse rate of $-.65K/100m$.

Inserting γ and Δ we get

$$\beta_p(f=1) = \frac{c_p}{\varepsilon L} \frac{(T_K - 35.85K)^2}{6.108hPa\, 17.27 \cdot 237.3K \exp\left(\frac{17.27(T_K - 273.15K)}{T_K - 35.85K}\right)} \times p_0 \left(\frac{T_K}{T_{0K}}\right)^{\frac{-g}{R\frac{\partial T_K}{\partial z}}} \tag{3.13}$$

with $T_K = T_{0K} + \frac{\partial T}{\partial z} z$. The maximum potential Bowen Ratio is the ratio of sensible to latent heat flux in case of 100% relative humidity. According to eq. (3.13) this ratio changes dramatically with elevation as shown in Figure 3.7. For elevations below about $3000m$ the potential Bowen ratio is smaller unity, indicating that the latent heat flux is larger than the sensible heat flux even in case of 100% humidity. Above that elevation the sensible heat flux becomes more important for the energy balance of the surface. Note that we talk about potential Bowen ratio, meaning that we talk about a water saturated surface without any resistance to evaporation.

We can conclude this section with the following statements:

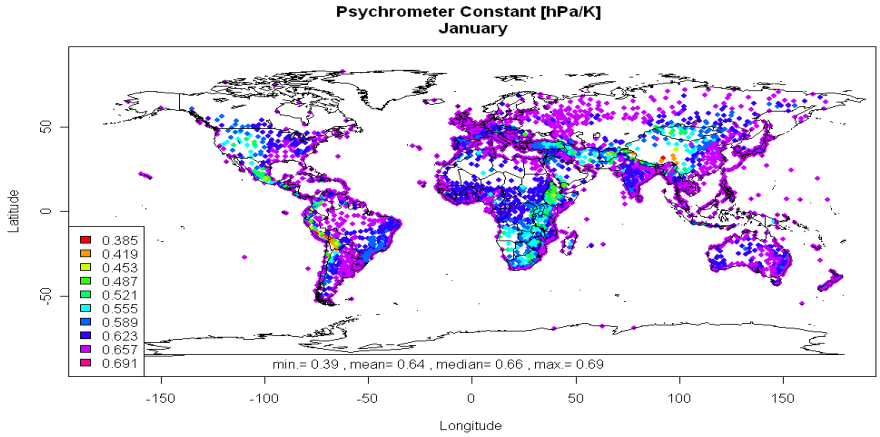

Figure 3.4: Map of psychrometric constant $\gamma \left[\frac{hPa}{K}\right]$ *from station observations, January.*

- the lower the relative humidity the higher the potential Bowen ratio,
- the higher the temperature the larger $\Delta(T)$ and $e_s(T)$ and thus the lower the potential Bowen ratio, and
- the higher a location, the lower p and T, the lower γ and Δ. Since $\frac{d\Delta}{dz} > \frac{d\gamma}{dz}$ the maximum potential Bowen ratio increases with height enhancing the fraction of sensible heat flux to total heat flux.

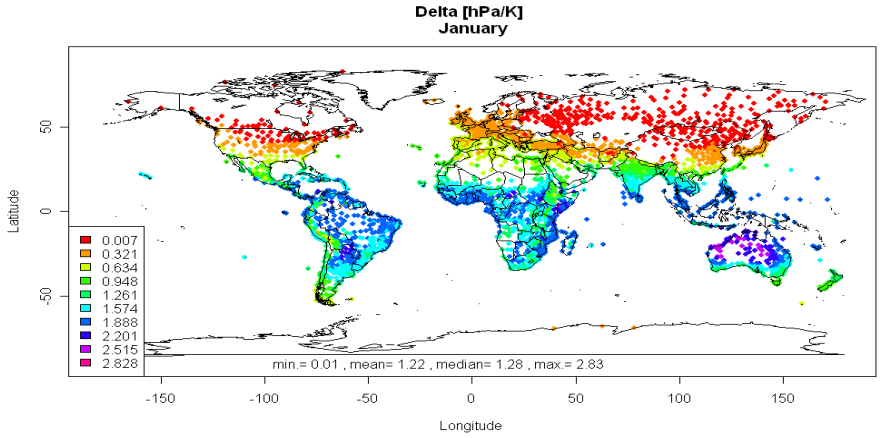

Figure 3.5: Maps of derivative of saturation vapor pressure $\Delta = \frac{de_s}{dT}\left[\frac{hPa}{K}\right]$ *from observations, January.*

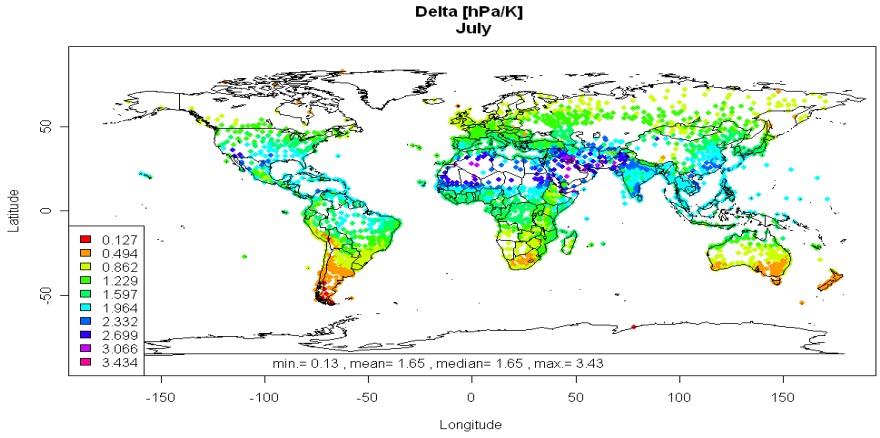

Figure 3.6: Maps of derivative of saturation vapor pressure $\Delta = \frac{de_s}{dT}\left[\frac{hPa}{K}\right]$ *from observations, July.*

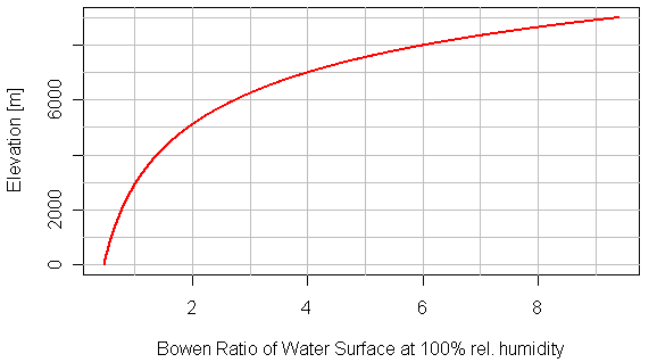

Figure 3.7: Maximum potential Bowen ratio $\frac{\gamma}{\Delta}$ as function of elevation.

Chapter 4

Approximations of PE

Several approximations to eq. (2.13) have been introduced. Some of them are described here.

4.1 Priestley-Taylor Method

They neglect the term $\frac{\alpha_H e_{2s}(1-f)}{\gamma+\Delta}$ and compensate this by a constant factor as

$$E_0|_{PT} = \frac{\Delta}{\gamma+\Delta}(Q_0 - G_0) \cdot 1.26. \tag{4.1}$$

4.2 Makkink's Approximation

Makkink further neglected the ground heat flow and the longwave radiation and again applied a correction factor as

$$E_0|_{Mk} = \frac{\Delta}{\gamma+\Delta}(1-\alpha)R_s \cdot 0.63 \tag{4.2}$$

where α is the surface albedo and R_s is the incoming solar radiation.

4.3 Hargreaves' Method

Hargreaves went a step further and approximated the incoming solar radiation by the extraterrestrial radiation supply R_a times a transmission factor which is only a function of daily maximum and minimum temperatures to get

$$E_0|_H = L \cdot \frac{0.0023}{^\circ C^{2/3}} \left(\frac{T_n + Tx}{2} + 17.8^\circ C\right) \cdot \sqrt{T_x - T_n} \cdot R_a \tag{4.3}$$

where the temperatures T_n and T_x are provided in $^\circ C$ and L is the latent heat of evaporation. Hargreaves' method is based on the close relation between atmospheric transmissivity and the square root of the daily temperature range as well as the mean daily temperature.

4.4 Blaney-Criddle Method

They averaged the extraterrestrial solar radiation by month and 5-degree latitude belt. Furthermore they assumed that the more radiation gets through the atmosphere the warmer it is. Therefore, their approximation is

$$E_0|_{BC} = C(\text{latitude, month}) \cdot (a + bT_m) \tag{4.4}$$

with the monthly mean temperature T_m.

4.5 Further Approximations

Further approximations, e.g. by Walter, Haude, Thornthwaite, Jensen and Haise, and Turc are even more empirically. They are often calibrated to data from a certain region and climate zone and thus should not be applied everywhere on Earth.

Chapter 5

Estimation of the transport coefficients

5.1 Bulk coefficients

In order to approximate the transport coefficients (α_H and α_W) the bulk method and the gradient method are combined. According to the bulk method eq. (2.2)) we have

$$H = -\alpha_H(\theta_2 - \theta_0) \tag{5.1}$$

The gradient method approximates local fluxes by their local gradients, e.g.

$$H = -\overline{\rho}\, c_p\, k_H(z)\frac{\partial\overline{\Theta}}{\partial z} \tag{5.2}$$

with the average density $\overline{\rho}$, the heat capacity c_p and the flux coefficient k_H. The latter has the dimension m^2/s. Eq. (5.2) can be integrated over z to get

$$\overline{\theta_2} - \overline{\theta_0} = \frac{H}{\overline{\rho}\, c_p}\int_{z_2}^{z_0}\frac{1}{k_H}dz \tag{5.3}$$

where we used the assumption that H does not depend on z, which is appropriate for the lowest atmospheric layer.

Inserting this into eq. (5.1) we get

$$\alpha_H = \frac{\rho\, c_p}{\int_{z_2}^{z_0}\frac{1}{k_H}dz}. \tag{5.4}$$

Furthermore we assume that the integral in the denominator only depends on the inverse wind speed in $z = 2m$ and get

$$\frac{1}{\int_{z_2}^{z_0}\frac{1}{k_H}dz} = C_H\overline{u_2} \tag{5.5}$$

with the drag coefficient for heat C_H and the average wind speed in 2m height $\overline{u_2}$ to get

$$\alpha_H = \rho\, c_p\, C_H \overline{u_2}. \tag{5.6}$$

Analog to that we can write

$$\alpha_W = \rho\, L\, C_W\, \overline{u_2} \tag{5.7}$$

and for the momentum

$$\alpha_M = \rho\, C_M\, \overline{u_2}. \tag{5.8}$$

This means that in case of $u_2 = 0$ no vertical flux of moisture, heat and momentum occurs due to the absence of turbulence. While this is in line with eq. (2.2) it does not hold in nature, where turbulence can also be generated thermally. According to eq. (2.14) only the ventilation term of evapotranspiration vanishes in case of $u_2 = 0$.

The coefficients C and α are often called bulk coefficients. The C's are dimensionless. And for $C_H = C_W$ we get $k_H = k_W$ and $\alpha_W = \alpha_H \cdot L/c_p$. The dimensions of the α's are

$$[\alpha_H] = \frac{W}{m^2 K},\ [\alpha_W] = \frac{W}{m^2},\ \text{and}\ [\alpha_M] = \frac{kg}{m^2}. \tag{5.9}$$

5.2 Resistance

According to Ohm's Law the bulk-flux relations can also be written in terms of resistances as

$$\begin{array}{rcll} H_0 &=& \alpha_H(\overline{\theta_0} - \overline{\theta_2}) &= \frac{1}{r_H}\overline{\rho}\, c_p(\overline{\theta_0} - \overline{\theta_2}) \quad \text{with} \quad r_H = \frac{\overline{\rho}\, c_p}{\alpha_H} = \frac{1}{C_H \overline{u_2}} \\ E_0 &=& \alpha_W(\overline{q_0} - \overline{q_2}) &= \frac{1}{r_W}\overline{\rho}\, c_p(\overline{q_0} - \overline{q_2}) \quad \text{with} \quad r_W = \frac{\overline{\rho}\, L}{\alpha_W} = \frac{1}{C_W \overline{u_2}} \\ \tau_0 &=& -\alpha_M \overline{u_2} &= -\overline{\rho}\frac{\overline{u_2}}{r_M} \quad \text{with} \quad r_M = \frac{\overline{\rho}}{\alpha_M} = \frac{1}{C_M \overline{u_2}} \end{array} \tag{5.10}$$

The resistances r_H, r_W, and r_M have the units s/m. The higher the wind speed in $2m$ the lower is the atmospheric resistance for vertical fluxes of moisture, heat and momentum.

5.3 Atmospheric Resistance

It is often assumed that $r_H = r_W = r_A$, with the atmospheric resistance r_A. One formula used to estimate it in case of a crop canopy is

$$r_A = \frac{\ln\left(\frac{z_m - d}{z_{0m}}\right) \ln\left(\frac{z_h - d}{z_{0h}}\right)}{k^2 u_m} = \frac{1}{C_H\, u_2} \tag{5.11}$$

with

$$\begin{array}{rcl} z_m &=& \text{anemometer height } [m] \\ z_{0m} &=& \text{roughness length for momentum } [m] \\ z_h &=& \text{thermometer height } [m] \\ z_{0h} &=& \text{roughness length for heat and moisture } [m] \\ d &=& \text{displacement height } [m] \\ k &=& \text{von Karman constant } = 0.41 \\ u_m &=& \text{observed wind speed [m/s].} \end{array} \tag{5.12}$$

The displacement height d marks the zero level from which altitude above ground should be measured in case there is a canopy.

For a wide range of crops the following approximations are used:

$$\begin{aligned} d &= 2/3h \\ z_{0m} &= 0.123h \\ z_{0h} &= 0.1z_{0m} \end{aligned} \tag{5.13}$$

where h denotes the canopy height of the crop.

If we assume a grass of $12cm$ height and thermometer and anemometer heights of $2m$ we get $d = 0.08m$, $z_{0m} = 0.01476m$, $z_{0h} = 0.001476$ and

$$r_A \approx \frac{208}{u_2}. \tag{5.14}$$

Figure 5.1 shows the strong influence of wind speed on atmospheric resistance especially for low wind speeds. Low wind speeds cause little turbulence and thus little vertical exchange of air which weakens evaporation dramatically.

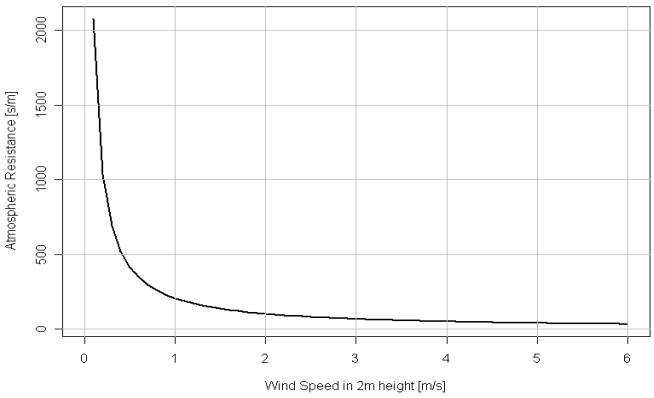

Figure 5.1: Atmospheric resistance [s/m] to evaporation as function of wind speed [m/s].

Chapter 6

The Influence of the Surface

6.1 Introduction of Surface Resistance

Using the atmospheric resistance r_A we can rewrite eq. (2.5) in form of Ohm's Law as

$$E_0 = \frac{\overline{\rho}\, L}{\gamma} \frac{e_0 - e_2}{r_A}. \tag{6.1}$$

This form allows to introduce the surface resistance r_S (soil surface and stomata of leaves) by assuming that these resistances add to the atmospheric resistance r_A like a sequence of resistances in an electric circuit as

$$E_0 = \frac{\overline{\rho}\, L}{\gamma} \frac{e_0 - e_2}{r_A + r_S}. \tag{6.2}$$

Assuming that there is no surface resistance to sensible heat flux we can further write

$$Q_0 - G_0 - \frac{\rho\, c_p}{r_A}(T_0 - T_2) - E_0 = 0. \tag{6.3}$$

We can insert eq. (6.2) and with the same approximations as in section 2.2 we get

$$E_0 = \frac{\Delta(Q_0 - G_0) + e_{2s} \frac{\rho\, c_p}{r_A}(1 - f)}{\Delta + \gamma \left(1 + \frac{r_S}{r_A}\right)}. \tag{6.4}$$

Finally, with $r_A = 1/(C_H\, u_2)$ we get

$$E_0 = \frac{\Delta(Q_0 - G_0) + e_{2s} \rho\, c_p\, C_H\, u_2 (1 - f)}{\Delta + \gamma\, (1 + r_S\, C_H\, u_2)} \tag{6.5}$$

and the only parameter left to estimate is the surface resistance r_S.

6.1.1 Estimation of Surface Resistance

The surface resistance r_S is influenced by many factors. Usually empirical relations are used for the estimation. One is

$$r_S = \frac{r_{S,min}}{LAI\, F_1\, F_2\, F_3\, F_4} \tag{6.6}$$

with

$$\begin{aligned} r_{S,min} &= \text{minimum surface resistance} \\ LAI &= \text{leaf area index} \\ F_1 &= \text{influence of photosynthetic radiation} \\ F_2 &= \text{influence of soil moisture} \\ F_3 &= \text{influence of air humidity} \\ F_4 &= \text{influence of air temperature} \end{aligned} \tag{6.7}$$

Another empirical relation is

$$r_S = \frac{r_l}{LAI_{act}} \tag{6.8}$$

with

$$\begin{aligned} r_l &= \text{plant specific bulk stomatal resistance} \\ LAI_{act} &= \text{active leaf area index.} \end{aligned} \tag{6.9}$$

For reference grass the following relations apply

$$\begin{aligned} LAI_{act} &= 0.5\, LAI, \\ LAI &= 24/m \cdot h \text{ and} \\ r_{l,grass} &= 100 s/m \text{ for well watered grass.} \end{aligned} \tag{6.10}$$

The surface resistance of a $12cm$ high reference grass is therefore $r_S \approx 70 s/m$.

Chapter 7

Grass Reference Evapotranspiration ETo

The evaporation of the standard grass with a depth of $0.12m$, a surface resistance of $70s/m$ and an albedo of 0.23 is called grass reference evapotranspiration ETo. In order to achieve ETo we first divide eq. (6.4) by the latent heat of evaporation L, insert $r_S = 70m/s$ and $r_A = 208/u_2$ and get

$$ETo = \frac{\Delta/L(Q_0 - G_0) + e_{2s}\frac{\rho\, c_p\, u_2}{208 \cdot L}(1-f)}{\Delta + \gamma\left(1 + \frac{70\, u_2}{208}\right)} = ETo_{Rad} + ETo_{Vent}. \tag{7.1}$$

with

$$\begin{aligned} ETo_{Rad} &= \frac{\Delta/L(Q_0-G_0)}{\Delta+\gamma\left(1+\frac{70\, u_2}{208}\right)} \\ ETo_{Vent} &= \frac{e_{2s}\frac{\rho\, c_p\, u_2}{208\cdot L}(1-f)}{\Delta+\gamma\left(1+\frac{70\, u_2}{208}\right)}. \end{aligned} \tag{7.2}$$

The lower the wind speed the higher is the atmospheric resistance. For $u_2 = 0$ the ventilation term vanishes completely and ETo is solely driven by the radiation term

$$ETo(u_2 = 0) = ETo_{Rad}(u_2 = 0) = \frac{\Delta(Q_0 - G_0)}{L(\Delta + \gamma)}. \tag{7.3}$$

The ventilation term also vanishes in case that relative humidity reaches 100%. In this case ETo becomes

$$ETo(f = 1) = ETo_{Rad} = \frac{\Delta(Q_0 - G_0)}{L\left(\Delta + \gamma\left(1 + \frac{70\, u_2}{208}\right)\right)}. \tag{7.4}$$

We can rewrite eq. (7.1) by using $c_p = \gamma\varepsilon\, L/p$ and $p = \rho\, T_v\, R$ with the gas constant for dry air $R = 287J/kg/K$, the approximated virtual temperature $T_v \approx 1.01 \cdot T$, the ratio $\varepsilon = 0.622$ of molecular weight of water vapor to dry air and the latent heat of evaporation $L = 2.45MJ/kg$ to get

$$\frac{\rho\, c_p\, u_2}{208 \cdot\ L} = \frac{\gamma\varepsilon\, u_2}{1.01\, T\, R\, 208} \approx \frac{\gamma 0.622 u_2}{1.01 \cdot T\, 287J/kg/K \cdot 208}. \tag{7.5}$$

The virtual temperature T_v is defined as

$$T_v = \left(1 + \left(\frac{R_v}{R_d} - 1\right) q\right) T \tag{7.6}$$

with the gas constant for water vapor $R_v = 461 \frac{J}{kg\,K}$, the gas constant for dry air $R_d = 287 \frac{J}{kg\,K}$ and the specific humidity q in kg water vapor per kg air. With $\left(\frac{R_v}{R_d} - 1\right) \approx 0.606$ we see immediately that the approximation $T_v = 1.01 \cdot T$ is exact in case of $16.5g$ water vapor per kg air. T_v converges against T in case of very low humidity and $T_v = 1.02 \cdot T$ in case of $q = 33 \frac{g}{kg}$. In both cases the approximation above has a relative error of about 1%.

The SI units of evaporation are $kg/m^2/s$ which in case of water can be translated to mm/s. Meteorologists, however, prefer using mm/day. This can easily be achieved by inserting $(Q_0 - G_0)$ in MJ/day and multiplying the second term by $60 * 60 * 24 s/day$. Since we provide γ in hPa/K, we also need to express R_d in $hJ/kg/K$. Doing that we get

$$\begin{aligned} \frac{\rho\, c_p\, u_2}{208 \cdot L} &\approx \frac{\gamma 0.622 u_2}{1.01 \cdot T \cdot 2.87 \cdot hJ/kG/K 208} * 86400 s/day \\ &\approx \frac{\gamma u_2}{T}\, 89.1 \frac{mm\, s\, K^2}{day\, m\, hPa}. \end{aligned} \tag{7.7}$$

Finally we get

$$ETo = \frac{.408 \frac{kg}{MJ} \Delta (Q_0 - G_0) + e_{2s} \gamma \frac{90}{T} u_2 (1 - f)}{\Delta + \gamma \left(1 + 0.34 \frac{s}{m}\, u_2\right)} \tag{7.8}$$

and keep in mind that γ and Δ are provided in hPa/K. This is the FAO version of ETo.

In order to shortly discuss the importance of wind and elevation, we have a closer look at $a = \frac{\Delta}{\Delta + \gamma(1 + .34 u_2)}$ and $b = \frac{\gamma}{\Delta + \gamma(1 + .34 u_2)}$. We can interpret a and b as the weights that are attributed to the influence of radiation and humidity on evaporation. If we assume $u_2 = 0$ the terms reduce to $\frac{\Delta}{\Delta + \gamma}$ and $\frac{\gamma}{\Delta + \gamma}$, respectively. In this case a and b are the fractions attributed to each term. However, in this case the influence of humidity vanishes anyway due to $u_2 = 0$. Without wind, evaporation is solely driven by radiation. The evaporation rate decreases with elevation even if the radiation balance is the same due to the decrease of $\frac{\Delta}{\Delta + \gamma}$ with elevation as depicted in Figure 7.1.

In case, that there is wind, the weights of radiation-driven and humidity-driven evaporation change with elevation. This is shown in Figure 7.2. This figure should be treated with care since not only γ and Δ change with elevation. Part of the radiation term goes with $-T^4$ while the ventilation term is proportional $1/T$. A more detailed analysis is subject of a later section.

Fig. 7.3 shows how the denominator of ETo depends on elevation. However, γ and Δ are also part of the numerator. As a result only the weights shift from the radiation term to the ventilation term.

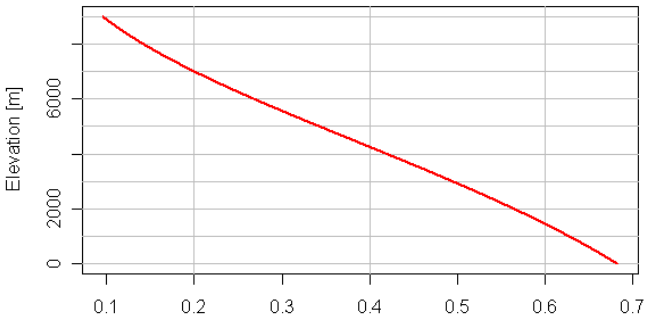

Figure 7.1: Dependence of $\frac{\Delta}{\Delta+\gamma}$ on elevation.

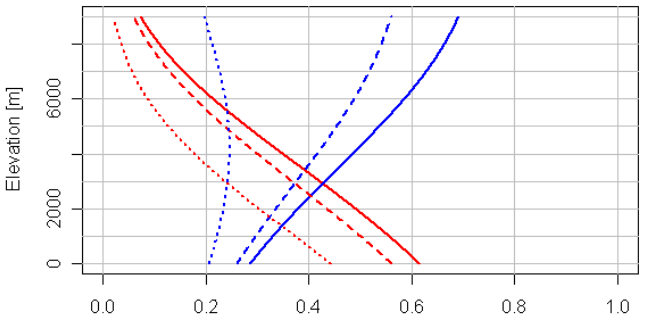

Figure 7.2: Dependence of $\frac{\Delta}{\Delta+\gamma\cdot(1+0.34u_2)}$ (red lines) and $\frac{\gamma}{\Delta+\gamma\cdot(1+0.34u_2}$ (blue lines) for $u_2 = 1m/s$ (solid lines), $u_2 = 2m/s$ (dashed lines), $u_2 = 4m/s$ (dotted lines) on elevation.

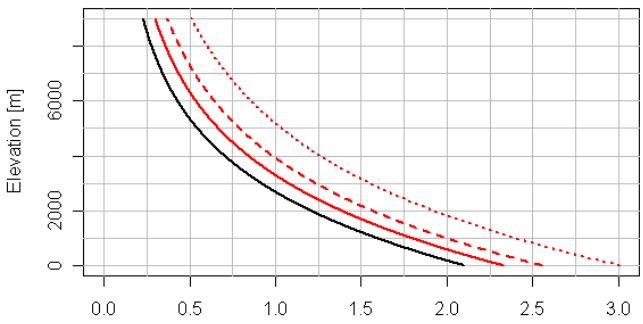

Figure 7.3: Dependence of the denominator of ETo ($\Delta + \gamma \cdot 0.34u_2$) in case of $u_2 = 0$ (black line), $u_2 = 1m/s$ (solid red line), $u_2 = 2m/s$ (dashed red line), $u_2 = 4m/s$ (dotted red line) on elevation.

Chapter 8

Parameterization of Radiation

8.1 Extraterrestrial Radiation

The extraterrestrial radiation R_a is given by

$$R_a = \frac{G_s\, d_r}{\pi} \left(\omega_s \sin\varphi \sin\delta + \cos\varphi \cos\delta \sin\omega_s\right) \tag{8.1}$$

with the solar constant $G_s = 0.082 MJ/m^2/day$, the solar declination

$$\delta = 0.409 \sin\left(\frac{2\pi\, J}{365} - 1.39\right) \tag{8.2}$$

and the Julian day J, as well as the inverse relative distance between the sun and the earth

$$d_r = 1 + 0.033 \cos\frac{2\pi\, J}{365}, \tag{8.3}$$

the latitude φ and the sunset-hour angle

$$\omega_s = \mathrm{acos}(-\tan\varphi \cdot \tan\delta). \tag{8.4}$$

8.2 Shortwave Radiation Balance

The shortwave radiation reaching the ground depends on the sunshine hours n. For clear-sky conditions the day length

$$N = \frac{24}{\pi}\omega_s \tag{8.5}$$

is the number of sunshine hours. Generally the incoming short-wave radiation at the ground R_s is linearly parameterized as function of the sunshine fraction n/N as

$$R_s = \left(a_s + b_s \frac{n}{N}\right) R_a \tag{8.6}$$

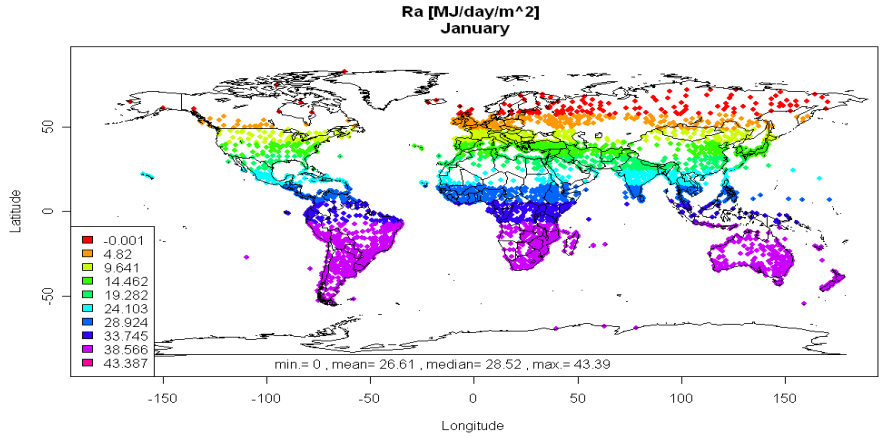

Figure 8.1: Extraterrestrial radiation $R_a \left[\frac{MJ}{m^2 day}\right]$*, January.*

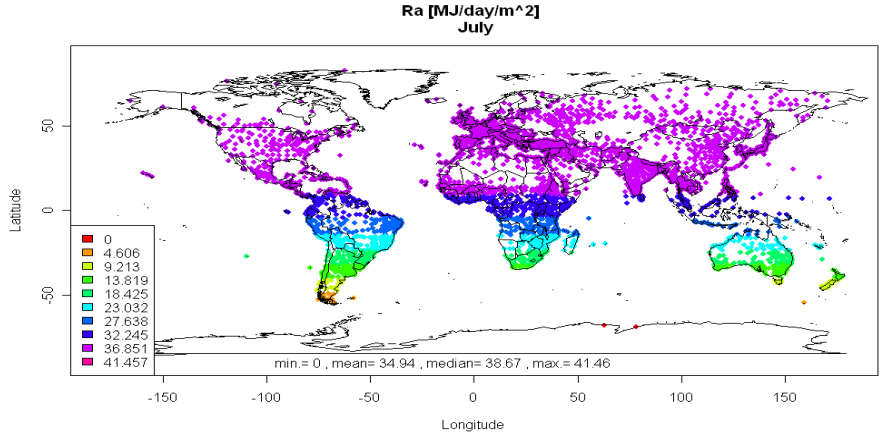

Figure 8.2: Extraterrestrial radiation $R_a \left[\frac{MJ}{m^2 day}\right]$*, July.*

with the Angstrom coefficients a_s and b_s. These coefficients are set to $a_s = 0.25$ and $b_s = 0.5$ if no local observations are available. It follows directly that under clear-sky conditions the incoming shortwave radiation at the surface is

$$R_{s0} = (a_s + b_s)R_a. \tag{8.7}$$

However, at higher elevations incoming solar radiation has to go through a smaller fraction of the atmosphere which is dryer and usually contains less aerosol particles than lower atmospheric layers. Therefore clear-sky solar radiation is often modeled as function of elevation, e.g. as

$$R_{s0} = (a_s + b_s + 2 \cdot 10^{-5} z)R_a. \tag{8.8}$$

Comparing eq. (8.6) and eq. (8.8) we see that the clear-sky radiation is taken to be increasing with increasing elevation, while the incoming shortwave radiation at the surface is not.

The shortwave net radiation (or shortwave radiation balance) is the difference of the incoming solar radiation and the reflected fraction of it given by the surface albedo

(which is $\alpha = 0.23$ in case of reference grass). The net solar radiation is therefore

$$R_{ns} = (1 - \alpha)\, R_s. \tag{8.9}$$

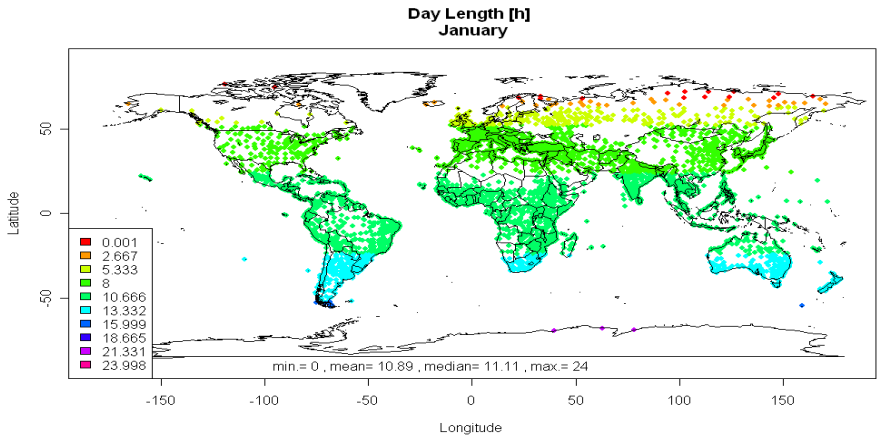

Figure 8.3: Day length $N[h]$, January.

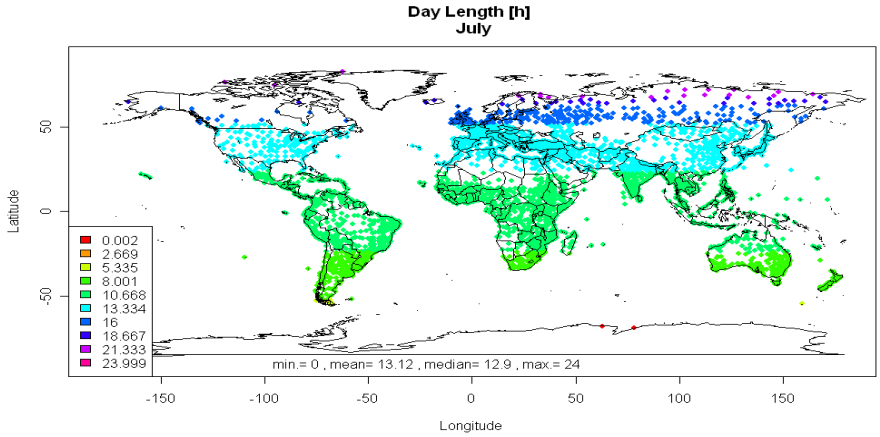

Figure 8.4: Day length $N[h]$, July.

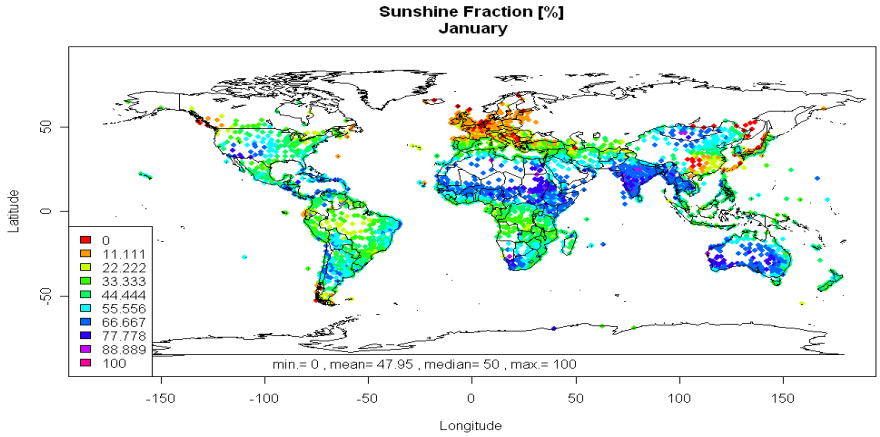

Figure 8.5: Sunshine fraction nN [%] January.

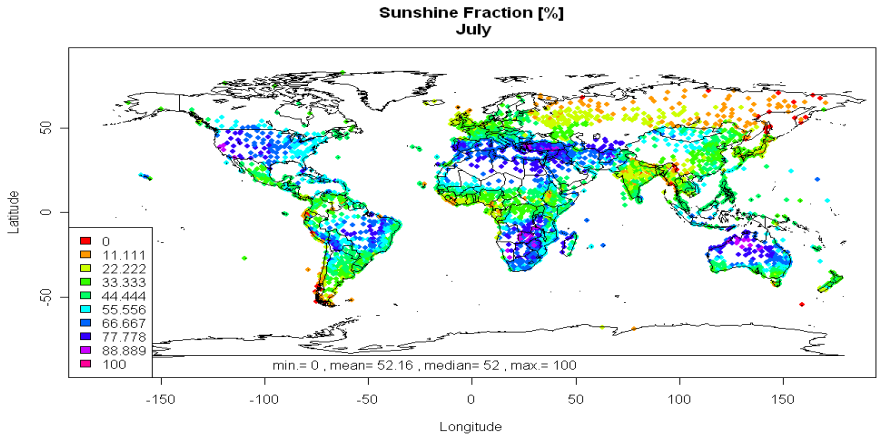

Figure 8.6: Sunshine fraction nN [%] July.

8.3 Longwave Radiation Balance

According to the Stefan-Boltzmann Law the outgoing radiation from the surface is proportional to the temperature to the power of 4 and the Stefan-Boltzmann constant $\sigma = 5.67 \times 10^{-8} \frac{W}{m^2 K} = 4.903 \times 10^{-9} \frac{MJ}{m^2 K^4}$. However, part of it is re-radiated from the atmosphere to the ground, which is called greenhouse effect. The largest contribution to this greenhouse effect is due to water vapor and clouds. This is why two feedback coefficients are included in the net long-wave radiation

$$R_{nl} = \sigma T^4 \times C_v \times C_c \tag{8.10}$$

with the empirical water vapor feedback coefficient

$$C_v = 0.34 - 0.14\sqrt{e_a/10hPa} \tag{8.11}$$

as well as the empirical cloud feedback coefficient

$$C_c = 1.35\frac{R_s}{R_{s0}} - .35 \tag{8.12}$$

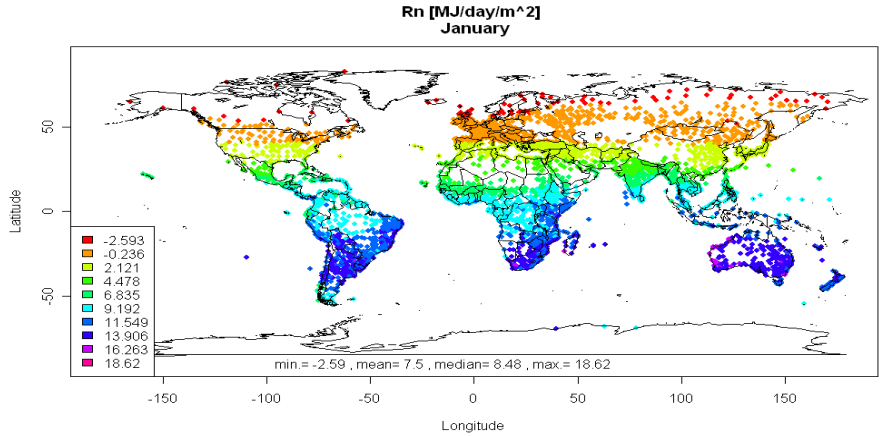

Figure 8.7: Incoming solar radiation at the surface R_s $\left[\frac{MJ}{m^2 day}\right]$, *January.*

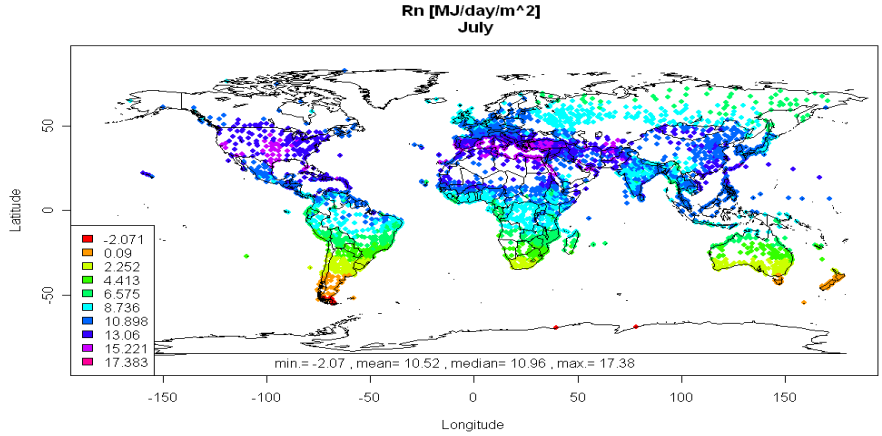

Figure 8.8: Incoming solar radiation at the surface R_s $\left[\frac{MJ}{m^2 day}\right]$, *July.*

where the latter is limited to be smaller unity. Fig. 8.11 shows that even high water vapor pressures do reduce the outgoing longwave radiation only by about 20% (i.e. from .34 to .28) while cloud cover can have a much stronger effect. A sunshine fraction of zero reduces the outgoing longwave radiation by 90% compared to clearsky conditions.

For daily data R_{nl} is usually estimated by using daily maximum and minimum temperatures, For monthly data monthly averaged daily maximum and minimum temperatures, $\overline{T_x}$ and $\overline{T_n}$ are used, respectively, and the results are arithmetically averaged, yielding

$$R_{nl} = \sigma \frac{(T_x^4 + T_n^4)}{2} \times C_v \times C_c. \tag{8.13}$$

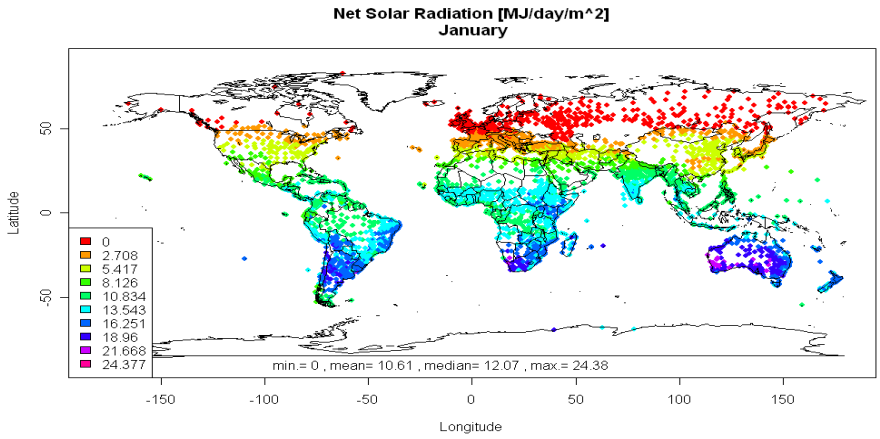

Figure 8.9: Net solar radiation at the surface R_{ns} $\left[\frac{MJ}{m^2 day}\right]$, *January.*

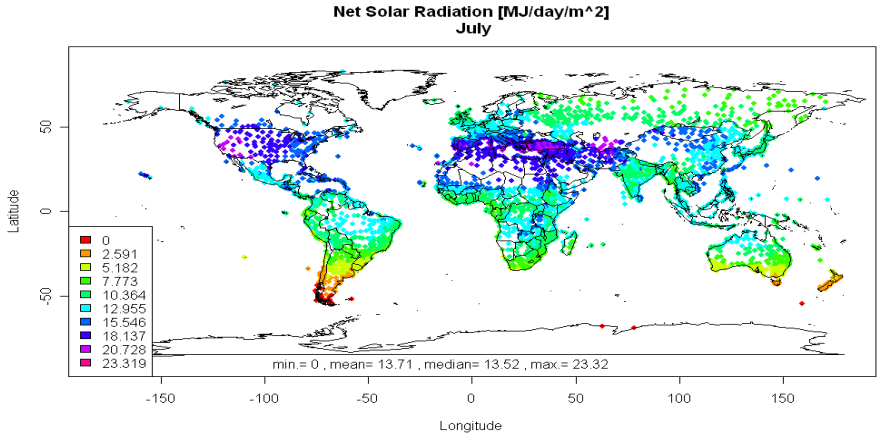

Figure 8.10: Net solar radiation at the surface R_{ns} $\left[\frac{MJ}{m^2 day}\right]$, *July.*

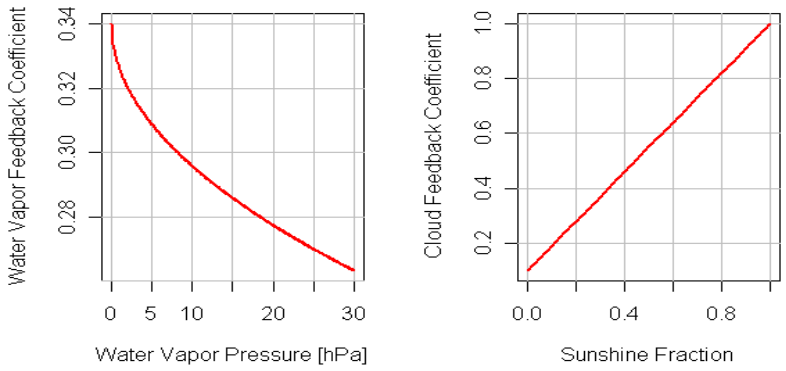

Figure 8.11: Feedback coefficients for long-wave radiation from water vapor (right plot) and from cloud cover (left plot).

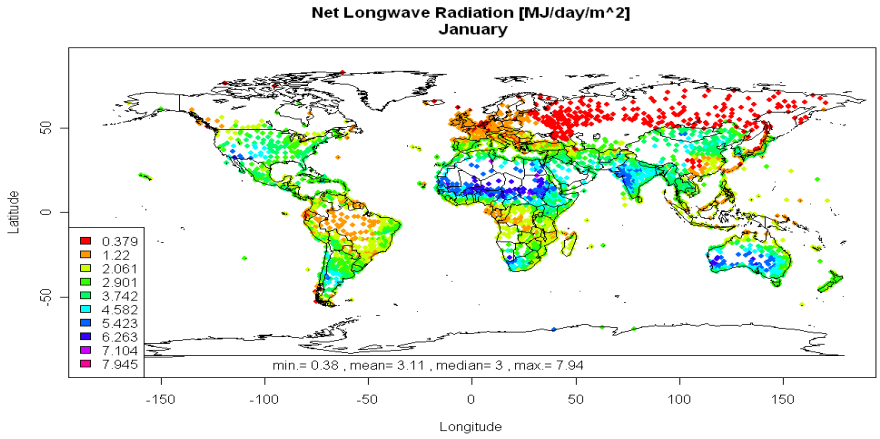

Figure 8.12: Net longwave radiation at the surface R_{nl} $\left[\frac{MJ}{m^2 day}\right]$, *January.*

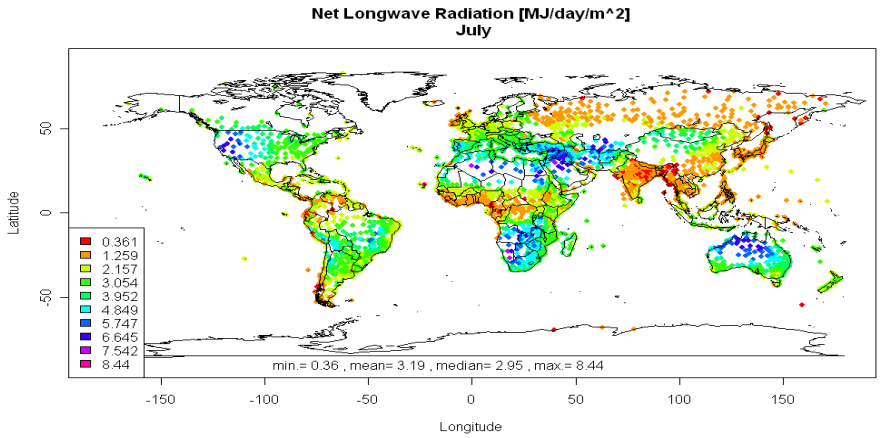

Figure 8.13: Net longwave radiation at the surface Rnl $\left[\frac{MJ}{m^2 day}\right]$, *July.*

Chapter 9

Ground Heat Flux

The ground heat flux G within the time interval Δt is given as

$$G = c_s \frac{T_2 - T_1}{\Delta t} \Delta z \tag{9.1}$$

with the air temperature at the beginning and end of Δt, T_1 and T_2, respectively, the soil heat capacity c_s which is about $2.1 \frac{MJ}{m^3 K}$ and the effective soil depth Δz. With an effective soil depth of about $1m$ we get

$$G = 0.07 \frac{MJ}{m^2 K} (T_{m+1} - T_{m-1}) \tag{9.2}$$

for the monthly ground heat flux. For daily data the ground heat flux is usually neglected.

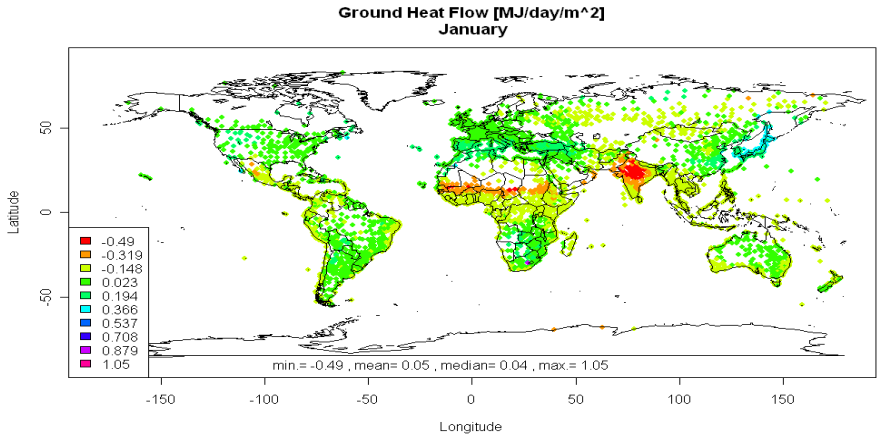

Figure 9.1: Ground heat flux G $\left[\frac{MJ}{m^2 day}\right]$*, January.*

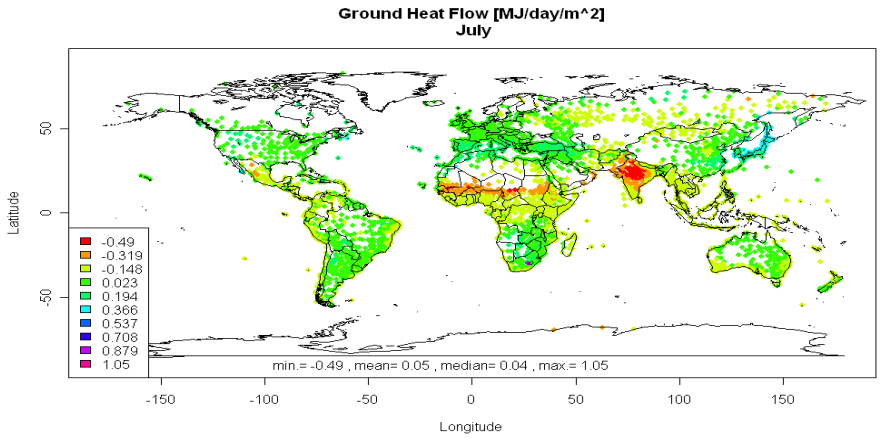

Figure 9.2: Ground heat flux G $\left[\frac{MJ}{m^2 day}\right]$*, July.*

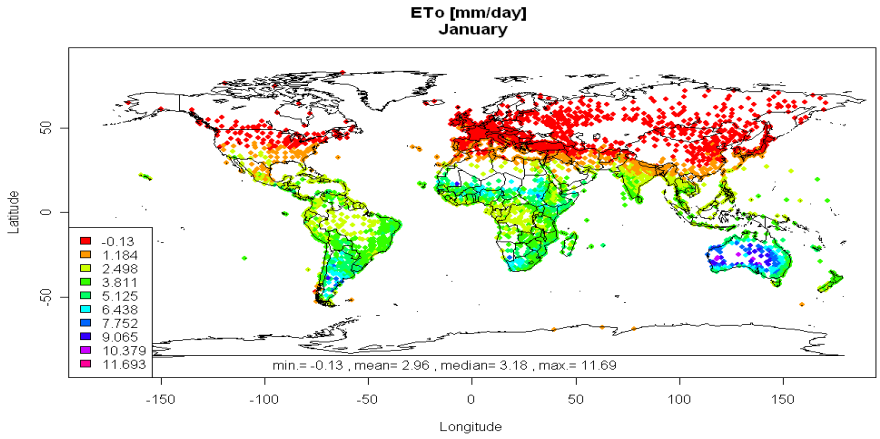

Figure 9.3: ETo $\left[\frac{mm}{day}\right]$*, January.*

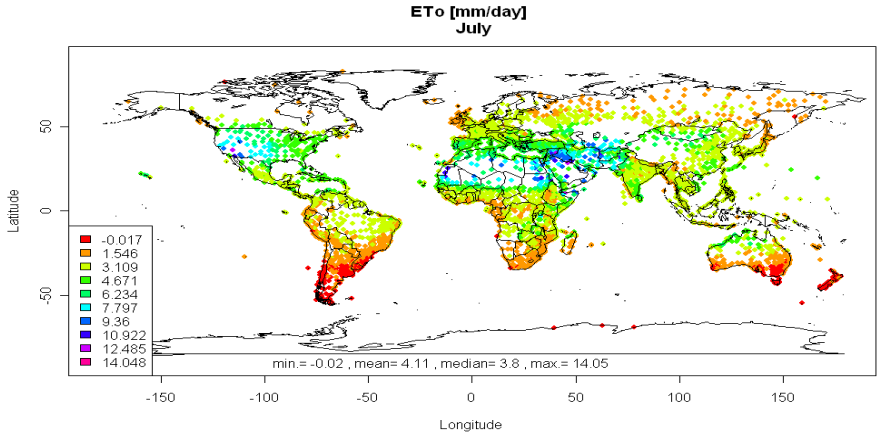

Figure 9.4: ETo $\left[\frac{mm}{day}\right]$*, July.*

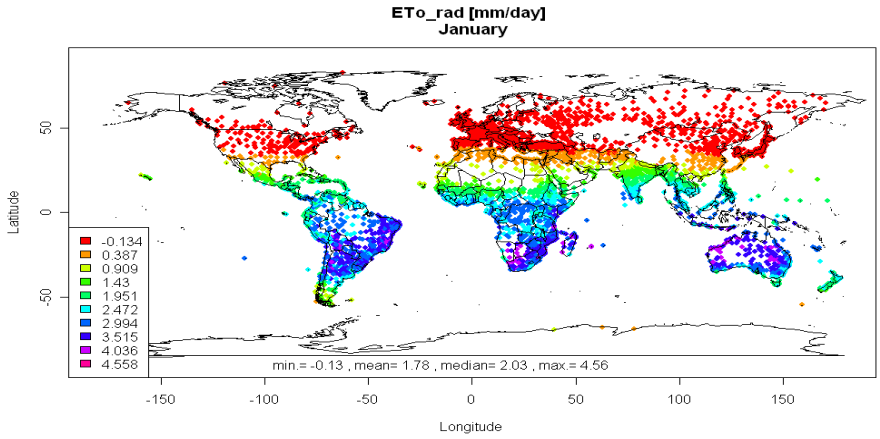

Figure 9.5: Radiation term of ETo $\left[\frac{mm}{day}\right]$*, January.*

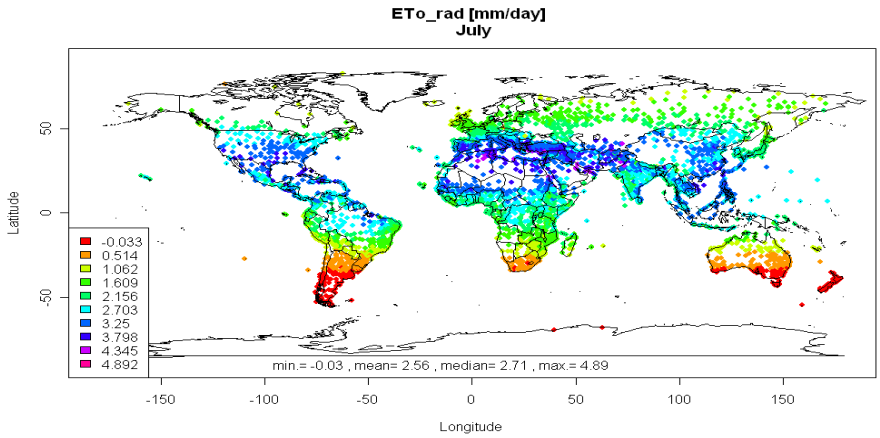

Figure 9.6: Radiation term of ETo $\left[\frac{mm}{day}\right]$*, July.*

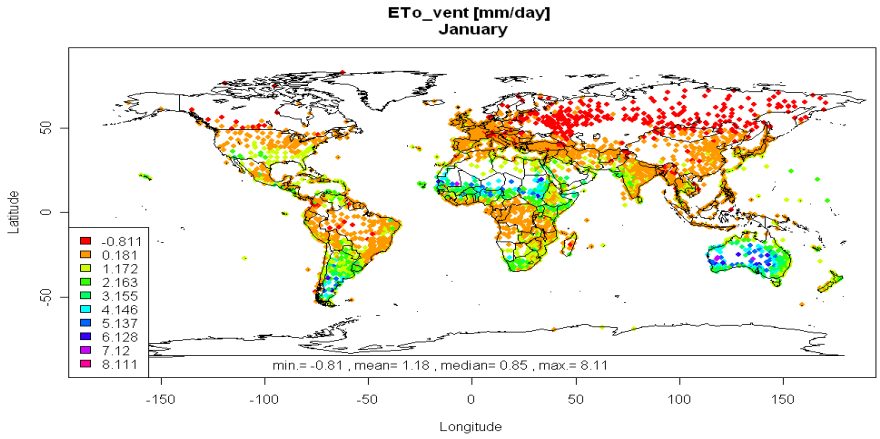

Figure 9.7: Ventilation term of ETo $\left[\frac{mm}{day}\right]$*, January.*

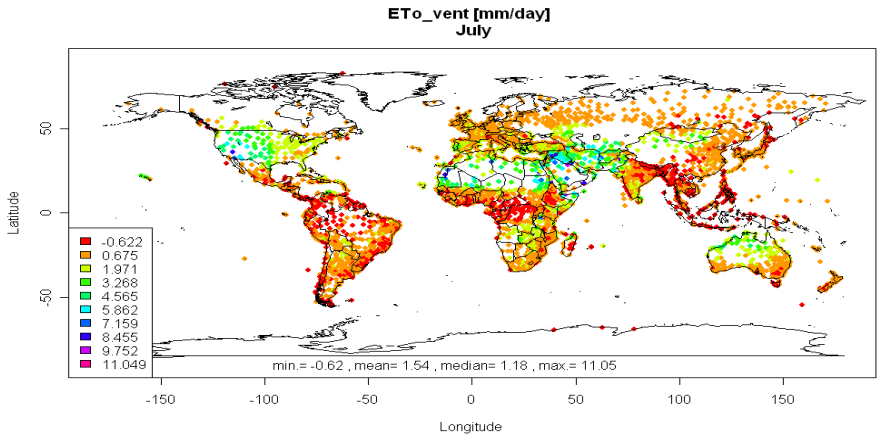

Figure 9.8: Ventilation term of ETo $\left[\frac{mm}{day}\right]$*, July.*

Chapter 10

Averages instead of Instantaneous Observations

10.1 Introduction

ETo is often not applied to instantaneous observations, though the equation is derived from principles which hold for each instant. Instead ETo is usually calculated on basis of daily or monthly means. However, a nonlinear function like ETo need not to produce reliable results if applied to averages in case of high variability.

In order to cope with this problem, FAO ETo uses $\frac{T_n^4+T_x^4}{2}$ instead of the mean temperature T_m^4 and estimates $e_s = \frac{e_s(T_n)+e_s(T_x)}{2}$ instead of $e_s(T_m)$. In general this can be formulated as

$$\overline{f_{NL}(T)} = \frac{f_{NL}(T_n) + f_{NL}(T_x)}{2} \neq f_{NL}(\overline{T}) \tag{10.1}$$

Now several questions arise. First, how wrong is the approximation used by FAO ETo? Second, how wrong is it to simply apply ETo on averages? Third, does it help to use knowledge about the variability of T? We know that temperature is a cyclo-stationary variable with period length of one day and one year.

We first discuss the highest possible error of longwave radiation and e_s with respect to the range of variability of T. Afterwards a more detailed error analysis is provided.

10.2 The highest possible error

Both, longwave radiation and saturation vapor pressure are monotonic functions $f_{NL}(T)$. Let us assume that T varies between its minimum T_n and its maximum T_x. In the worst case we know nothing about the way T varies between T_n and T_x. This means that we do not know the density distribution of T. So what is the highest error we can make? There are 2 possible extreme cases: T can be T_n for all of the time except an instant where it is T_x, or vice versa. In one case $f_{NL}(T_n)$ would do best, in the other case $f_{NL}(T_x)$. Therefore we can conclude that the true average $\overline{f_{NL}(T(t))}$ is limited by

$$f_{NL}(T_n) < \overline{f_{NL}(T(t))} < f_{NL}(T_x) \tag{10.2}$$

and the highest possible absolute error is $E = f_{NL}(T_x) - f_{NL}(T_n)$. Since f_{NL} is monotonically increasing the highest relative error becomes

$$\varepsilon = \frac{E}{f_{NL}(T_n)} = \frac{f_{NL}(T_x)}{f_{NL}(T_n)} - 1. \tag{10.3}$$

10.2.1 The highest possible error in outgoing longwave radiation

With the temperature range $\Delta = T_x - T_n$ equation (10.3) leads straight to

$$\begin{aligned} \varepsilon &= \frac{T_x^4}{T_n^4} - 1 \\ &= \frac{(T_n+\Delta)^4}{T_n^4} - 1 \\ &= 4\frac{\Delta}{T_n} + 6\frac{\Delta^2}{T_n^2} + 4\frac{\Delta^3}{T_n^3} + \frac{\Delta^4}{T_n^4} \end{aligned} \tag{10.4}$$

For minimum temperatures above $0°C$ T_n is larger $273K$. If we assume the diurnal range of temperature Δ to be below $27.3°C$ the ratio $\frac{\Delta}{T_N}$ is $< \frac{1}{10}$. Therefore we find that

$$\varepsilon < .4641 \tag{10.5}$$

which means that the highest possible error does not exceed 46%.

10.2.2 The highest possible error in saturation vapor pressure

Again we use the temperature range $\Delta = T_x - T_n$ to obtain

$$\varepsilon = \exp\left(b\frac{\Delta\, c}{T_n^2 + 2cT_n + \Delta T_n + c\Delta + c^2}\right) - 1. \tag{10.6}$$

Assuming $T_n = 0°C$ and $\Delta = 27.3°C$ we get

$$\varepsilon < 3.68 \tag{10.7}$$

which means that in this case the highest possible error reaches 368% which is about 8 times the highest possible error in outgoing longwave radiation.

We see that the estimation of the saturation vapor is much more sensitive to variability in temperature than it is the case with outgoing longwave radiation.

10.3 Taking periodicity into account

If there were no temperature variability than

$$T_n = \overline{T} = T_x. \tag{10.8}$$

However, usually there is a daily cycle which is assumed to be symmetric so that

$$\overline{T} = \frac{T_n + T_x}{2}. \tag{10.9}$$

The same symmetry is often assumed to hold true also for the derived variables leading to eq.(**??**). If temperatures were half day on the maximum and half day on the minimum then eq.(**??**) would no longer be an approximation but a true relation. In reality temperature varies periodically between maximum and minimum. Thus we could assume that eq.(**??**) is an overestimation while $f_{NL}(\overline{T})$ underestimates $\overline{f_{NL}(T)}$. We go deeper into the matter of periodic functions in the following section.

10.3.1 The daily cycle of outgoing longwave radiation

Let us assume that the daily temperature cycle can be described by a cosine function

$$T(t) = \overline{T} + \frac{\Delta}{2}\cos(2\pi t - \varphi), t \in \{0, 1\} \tag{10.10}$$

where φ is the phase shift that can be neglected as long as we are interested in daily means. In this case the true daily average of longwave outgoing radiation is

$$\overline{R_L} = \sigma \int_0^1 T(t)dt = \sigma \int_0^1 \left(\overline{T} + \frac{\Delta}{2}\cos(2\pi t - \varphi)\right)^4 dt \tag{10.11}$$

where the integral is from 0 to 1 which corresponds to the beginning and end of day. To keep things simple φ is set to 0. This does not affect the results. The integral can be solved straight forward leading to

$$\overline{R_L} = \sigma\overline{T}^4 + \frac{3}{4}\sigma\overline{T}^2\Delta^2 + \frac{3}{128}\sigma\Delta^4. \tag{10.12}$$

This true outgoing longwave radiation has to be compared to both the approximations resulting from using average or extremes, respectively. Using average temperature leads to

$$\overline{R_L} \approx \sigma\overline{T}^4 \tag{10.13}$$

while the use of extreme temperatures leads to

$$\begin{aligned} \overline{R_L} &\approx \sigma\frac{T_n^4 + T_x^4}{2} = \sigma\frac{(\overline{T} - \frac{\Delta}{2})^4 + (\overline{T} + \frac{\Delta}{2})^4}{2} \\ &\approx \sigma\left(\overline{T}^4 + \tfrac{6}{4}\overline{T}^2\Delta^2 + \tfrac{1}{16}\Delta^4\right). \end{aligned} \tag{10.14}$$

Since $\Delta < .1\overline{T}$ the terms containing Δ^4 can be neglected and we see

$$\sigma\overline{T}^4 \leq \sigma\left(\overline{T}^4 + \frac{3}{4}\overline{T}^2\Delta^2\right) \leq \sigma\left(\overline{T}^4 + \frac{6}{4}\overline{T}^2\Delta^2\right). \tag{10.15}$$

The absolute of the highest possible error in case of a cosine shaped daily cycle is

$$|\varepsilon| = \frac{3}{4}\frac{\Delta^2}{\overline{(T)}^2} < 1\%. \tag{10.16}$$

This can be considered to be a small error.

10.3.2 The daily cycle of saturation vapor pressure

The temperature may again follow a cosine. The daily cycle of saturation vapor pressure then is

$$\overline{e_s} = a \int_0^1 \exp\left(\frac{b\left(\overline{T} + \frac{\Delta}{2}\cos(2\pi t - \varphi)\right)}{\overline{T} + \frac{\Delta}{2}\cos(2\pi t - \varphi) + c}\right) dt. \tag{10.17}$$

Though this integral can be solved analytically it is too much effort here and alternatively numerical investigations are performed.

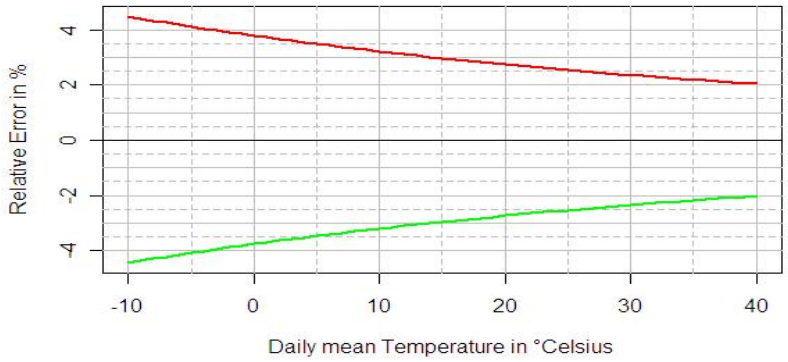

Figure 10.1: Average relative error in estimated saturation vapor pressure e_s as a function of daily mean temperature if the daily cycle of temperature follows a cosine and a) the daily mean temperature is used for the approximation (blue line) and b) the daily maximum and minimum temperatures are used for the approximation (red line). The average is taken over amplitudes of daily cycles of 0 to 20 degrees Celsius.

To get the exact average of saturation vapor pressure the integral is solved numerically for 41 average temperatures $\overline{T}$ from 0 degrees Celsius to 40 degrees Celsius and 21 diurnal temperature ranges from 0 degrees Celsius to 20 degrees Celsius (for simplicity only integer values of temperatures are taken). For all these 861 cases the exact average of saturation vapor pressure is compared to the estimates based on average temperature only and based on extreme temperatures only. Fig. 10.1 shows the average relative error as a function of the daily mean temperature. As expected the use of extreme temperatures overestimates $\overline{e_s}$ while the use of $\overline{T}$ underestimates the true saturation vapor pressure. However, the absolute of the error is roughly the same for both approximations. With increasing temperatures the relative error gets smaller since the relative amplitude of the diurnal cycle compared to the average temperature decreases with increasing mean temperature. Average errors are about 2% at 40 degrees Celsius and nearly 4% at 0 degrees Celsius.

Fig. 10.2 shows the dependence of the mean relative error from the diurnal temperature range since the amplitude of the diurnal cycle drives the influence of nonlinearity. Again it shows that both approximations provide equally good estimates with opposite sign. Errors vanish if there is no diurnal cycle and exceed 8% if the amplitude of the daily cycle approaches 20 degrees Celsius.

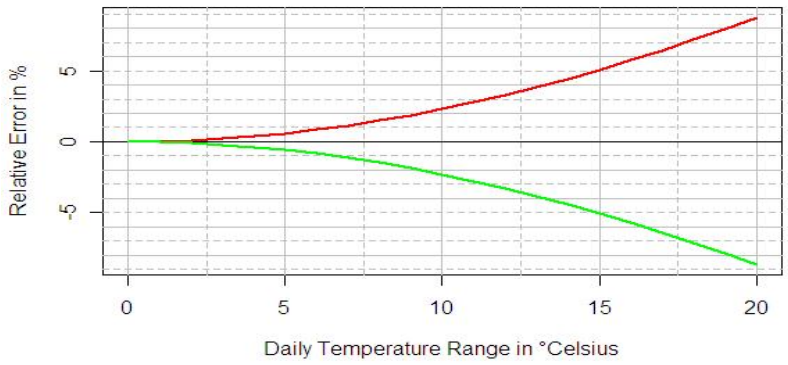

Figure 10.2: Average relative error in estimated saturation vapor pressure e_s as a function of the temperature amplitude of the daily cycle if it follows a cosine and a) the daily mean temperature is used for the approximation (green line) and b) the daily maximum and minimum temperatures are used for the approximation (red line). The average is taken over mean daily temperatures from 0 to 40 degrees Celsius.

We have seen that the Stefan-Boltzmann law is rather insensitive to the use of average or extremes of temperature. In case of a cosine daily temperature cycle the true average of outgoing longwave radiation is in the middle of both estimates. The error is below 1%.

Also in case of saturation vapor pressure both estimates are of nearly equal amplitude with opposite signs. However, the error can reach 8% which might be regarded as considerably high. The results suggest that for a daily cycle of cosine form the average of both approximations is pretty good.

However, true daily cycles are not like a cosine. Instead they might be regarded as a solution of a linear differential equation with a relaxation term of an order of between T and T^4 and a cosine forcing during daytime. An alnalytic solution of this equation that can be fit to the observed T_x and T_n might provide a better approximation.

10.4 An Example

We now calculate average ETo for April in Bangkok. This is example 17 in FAO56. The following observations are available:

$$\begin{aligned} T_n &= 25.6°C \\ T_x &= 34.8°C \\ T_m &= 30.2°C \\ T_{m,-1} &= 29.2°C \\ n &= 8.5\text{hrs} \\ u_2 &= 2m/s \\ e_a &= 28.5hPa. \end{aligned} \tag{10.18}$$

Given these data we get

$$\begin{aligned} e_{s1} &= e_s(\overline{T}) = 42.9hPa \\ e_{s2} &= \frac{e_s(T_n)+e_s(T_x)}{2} = 44.2hPa. \end{aligned} \tag{10.19}$$

For the net longwave radiation balance we get

$$\begin{aligned} R_{nl1} &= C_v\, C_c\, \sigma T_m^4 = 3.108 \frac{MJ}{m^2\, day} \\ R_{nl2} &= C_v\, C_c\, \sigma \frac{T_n^4+T_x^4}{2} = 3.104 \frac{MJ}{m^2\, day}. \end{aligned} \tag{10.20}$$

Table 10.1: Comparison of estimated ETo from FAO56 and by use of $ET_o(e_s(T_m)$ and $R_{nl}(T_m))$ for the case of Bangkok in April, as well as relative and absolute differences.

Variable	ETo(FAO56) $\left[\frac{mm}{day}\right]$	$ET_o(e_s(T_m)$, $R_{nl}(T_m))$ $\left[\frac{mm}{day}\right]$	Abs. Diff. $\left[\frac{mm}{day}\right]$	Rel. Diff. [%]
ETo_{rad}	3.9654	3.9666	-0.0012	-0.03
ETo_{vent}	1.7494	1.6049	0.1445	8.26
ETo	5.7149	5.5715	0.1433	2.51

Table 10.1 shows clearly that the use of means of extremes instead of simple means of temperature can make a difference in the range of percents. Since the influence on e_s is usually higher than on R_{nl} we can expect a higher influence on ETo in regions and seasons where the ventilation term is more important, i.e. in higher latitudes, during winter and where there are strong winds.

Chapter 11

Open Water Evaporation

One might be tempted to apply the potential evaporation equation directly to open water. However, this might result in an overestimation. While potential evaporation is based on the assumption of a radiative balance at the surface, we face the problem that radiation intrudes a water body, making the estimation of the energy balance of the surface much more difficult.

Generally, temperature differences between surface and 2m height are much less over sea than they are over land due to the low fraction of shortwave radiation absorbed by the water surface. Therefore wind and vapor pressure deficit play a much more important role over open water. According to Budyko (1974) the approach

$$E_w = (e_s - e_a)Y(u) \tag{11.1}$$

with the empirical wind factor $Y(u)$ is often used, where $Y(u)$ could be either $Y = a+bu$ or $Y \propto u^m$ with $m \in [0.5, 1]$. Again according to Budyko, Shuleikin was the first to obtain the relation

$$E_w = \chi \rho u (q_s - q). \tag{11.2}$$

On the base of eq. (2.13) we would write

$$E_w = \frac{1}{L} \frac{\alpha_H e_{2s}(1-f)}{\gamma + \Delta} \tag{11.3}$$

instead. With $\alpha_H = \rho\, c_p\, C_H\, u_2$ we get

$$E_w = \frac{1}{L} \frac{\rho\, c_p\, C_H}{\gamma + \Delta}\, u_2 e_{2s}(1-f). \tag{11.4}$$

Analog to eq. (5.11) we use here

$$C_H = \frac{k^2}{\left(\ln \frac{z-d}{z_0}\right)^2} \tag{11.5}$$

with $d = 0$ over water. The roughness of open water, expressed by the roughness length z_0 is a function of the wind speed. The higher the wind speed the rougher the sea surface. Usually small values like 10^{-4} to 10^{-3} are used. With $z_0 = 10^{-3}$ we get

$C_H(z = 10m) = 0.01825$ and $C_H(z = 2m) = 0.02212$. Using the ideal gas law, we can replace $\rho c_p/L$ by $\frac{\varepsilon\,\gamma}{R_d\,T_v}$ and get

$$E_w = \frac{\varepsilon\,\gamma\,C_H}{R_d\,T_v(\gamma + \Delta)}\,u_2\,e_{2s}(T)\,(1 - f). \tag{11.6}$$

This equation describes evaporation over water as function of humidity, wind speed and temperature. It neglects the direct influence of radiation and thus assumes deep water. Shallow water (e.g. 1 meter depth) or brown water (swamps), to the contrary, can get heated in the first meters of water depths due to absorption of incoming shortwave radiation. In this case the radiation term cannot be neglected.

Chapter 12

Sublimation of Ice and Snow Surfaces and Frozen Ground

In case of ice, snow or frozen ground we have to consider three features:

1. Sublimation has a higher latent heat of than evaporation. The latent heat of sublimation is about $L_I = 2.86 MJ/m^2$ and thus 16.7% higher than the latent heat of evaporation at $20^{circ}C$. This reduces evaporation given the same energy balance than a surface with liquid water availability.

2. The surface albedo of snow and ice is much higher than those of bare soil and other material (see appendix D). The albedo of fresh snow can reach 90% and is thus about 4 times higher than the albedo of FAO reference grass (23%).

3. The roughness of snow and ice is low compared to vegetated surfaces. The roughness length z_0 is in the order of $0.001m$ while it is higher for vegetated surfaces, e.g. $0.015m$ for FAO reference grass.

Chapter 13

Sensitivity of ETo and Global Change

ETo depends on

- humidity, expressed either as relative humidity f, as specific humidity q, or as water vapor pressure e,
- solar net radiation R_{ns}, which depends on the surface albedo α, the latitude φ, the time in the year, and the sunshine fraction n/N
- long wave net radiation, which depends on temperatures T_n and T_x, humidity and sunshine fraction,
- temperature, and
- wind speed.

We now try to investigate the sensitivity of ETo with respect to each of the meteorological parameters by building the partial derivatives with respect to each variable while leaving the others constant. Again we write ETo as a sum of radiation and ventilation term keeping in mind that both terms depend on several meteorological variables

$$\begin{aligned} ETo_{Rad} &= \frac{\Delta/L(Q_0-G_0)}{\Delta+\gamma(1+0.34\,u_2)} = ETo_{Rad}(T_n, T_x, R_s, e_a, \tfrac{n}{N}, u_2) \\ ETo_{Vent} &= \frac{\gamma\frac{90}{T}\,u_2\,(e_{2s}-e_a)}{\Delta+\gamma(1+0.34\,u_2)} = ETo_{Vent}(T_n, T_x, e_a, u_2). \end{aligned} \tag{13.1}$$

If we assume no changes in seasonality there are no changes in surface heat flux, i.e. $\frac{\partial G_0}{\partial T} = 0$ since the temperature difference between different months of the year stays constant.

We also set the psychrometric constant γ constant, assuming that the vertical lapse rate does not change.

According to eq. (3.11) Δ has the form

$$\Delta(T_K) = \frac{a}{(T_K-d)^2}\exp\left(\frac{b(T_K-c)}{T_K-d}\right) \tag{13.2}$$

with

$$\begin{aligned} a &= 25031.63hPa, \\ b &= 17.27, \\ c &= -273.15K, and \\ d &= -35.85K. \end{aligned} \tag{13.3}$$

Following some calculus (see appendix B) we get

$$\frac{d\Delta}{dT} = \frac{\Delta}{T-d}\left(\frac{b(c-d)}{T-d} - 2\right) \tag{13.4}$$

and with

$$\frac{dT}{dT_x} = \frac{dT}{dT_n} = \frac{1}{2} \tag{13.5}$$

we get

$$\frac{d\Delta}{dT_x} = \frac{\Delta}{T_x-d}\left(\frac{b(c-d)}{2(T_x-d)} - 1\right) \tag{13.6}$$

and

$$\frac{d\Delta}{dT_n} = \frac{\Delta}{T_n-d}\left(\frac{b(c-d)}{2(T_n-d)} - 1\right). \tag{13.7}$$

13.1 Temperature

Due to non-linearity, changes in minimum temperature have a different effect than changes in maximum temperature. This is the reason why a term like $\frac{\partial ETo}{\partial T}$ is not meaningful without further concretization. ETo can change even if T keeps constant since an increase in T_x of the same magnitude as a decrease in T_n result in no change in mean temperature but may have a strong effect on ETo. However, if we apply further conditions we can build a conditional derivative with T. In case that we restrict changes δ in T_n and in T_x to be small and identical, we get

$$\delta ETo = \frac{\partial ETo}{\partial T_n}\delta T_n + \frac{\partial ETo}{\partial T_x}\delta T_x = \left(\frac{\partial ETo}{\partial T_n}\frac{\partial T_n}{\partial T} + \frac{\partial ETo}{\partial T_x}\frac{\partial T_x}{\partial T}\right)\delta T. \tag{13.8}$$

Assuming $\delta T = \delta T_n = \delta T_x$ we get

$$\left.\frac{\partial ETo}{\partial T}\right|_{\delta T_n = \delta T_x} = \frac{\partial ETo}{\partial T_n} + \frac{\partial ETo}{\partial T_x}. \tag{13.9}$$

The symmetry of the equations for the longwave radiation (see eq. (8.13)) and the mean humidity with respect to minimum and maximum temperature allows, however, to discuss them together. From the definition of the mean temperature as arithmetic mean of the minimum and maximum temperature we get

$$\frac{\partial T}{\partial T_n} = \frac{\partial T}{\partial T_x} = \frac{1}{2} \tag{13.10}$$

We start with rewriting eq. (13.1) as

$$\begin{aligned} ETo_{Rad} &= \frac{\Delta/L(Q_0-G_0)}{\Delta+\gamma(1+0.34\,u_2)} = \frac{1}{L}\frac{\Delta\,(P-R_{nl}(T))}{\Delta(T)+Q} \\ ETo_{Vent} &= \frac{\gamma\frac{90}{T}\,u_2\,(e_s-e_a)}{\Delta+\gamma(1+0.34\,u_2)} = W\frac{e_s(T)-e_a}{\Delta(T)+Q} \end{aligned} \tag{13.11}$$

with

$$\begin{aligned} P &= R_{ns} - G_0 \\ Q &= \gamma\,(1 + 0.34\,u_2) \\ W &= \gamma \cdot 90 \cdot u_2. \end{aligned} \tag{13.12}$$

And after some calculus we get

$$\begin{aligned} \frac{\partial ETo_{Rad}}{\partial T_k} &= \frac{1}{L(\Delta+Q)^2}\left(Q\frac{d\Delta}{dT_k}(P - R_{nl}) - \Delta(\Delta + Q)\frac{dR_{nl}}{dT_k}\right) \\ \frac{\partial ETo_{Vent}}{\partial T_k} &= \frac{W}{T\,(\Delta+Q)}\left\{(e_a - e_s)\left(\frac{1}{2T} + \frac{1}{\Delta+Q}\frac{d\Delta}{dT_k}\right) + \frac{de_s}{dT_k}\right\} \end{aligned} \tag{13.13}$$

where the index k stands for maximum or minimum. Furthermore,

$$\frac{d\Delta}{dT_k} = \frac{d\Delta}{dT}\frac{\partial T}{\partial T_k} = \frac{1}{2}\frac{d\Delta(T)}{dT} \tag{13.14}$$

and

$$\frac{de_s}{dT_k} = \frac{de_s}{dT}\frac{\partial T}{\partial T_k} = \frac{1}{2}\Delta(T). \tag{13.15}$$

and finally

$$\frac{\partial ETo}{\partial T_k} = \frac{\partial ETo_{Rad}}{\partial T_k} + \frac{\partial ETo_{Vent}}{\partial T_k}. \tag{13.16}$$

13.2 Humidity

Both, the ventilation and the radiation term depend on humidity. With respect to water vapor pressure we get

$$\frac{\partial ETo}{\partial e_a} = \frac{\partial ETo_{Rad}}{\partial e_a} + \frac{\partial ETo_{Vent}}{\partial e_a} \tag{13.17}$$

The differentiation of the second term on the rhs is straight forward and yields

$$\frac{\partial ETo_{Vent}}{\partial e_a} = \frac{-\gamma\,90\,u_2}{T(\Delta + \gamma)(1 + 0.34u_2)}. \tag{13.18}$$

The differentiation of the radiation term can be written as

$$\frac{\partial ETo_{Rad}}{\partial e_a} = \frac{\partial ETo_{Rad}}{\partial R_{nl}}\frac{\partial R_{nl}}{\partial e_a} \tag{13.19}$$

where $\frac{\partial ETo_{Rad}}{\partial R_{nl}}$ is provided in section 13.3.2 and $\frac{\partial R_{nl}}{\partial e_a}$ in section 13.3.3.

In order to get the derivatives with respect to relative humidity we use $e_a = e_s \cdot \frac{f}{100}$ where f is expressed in % and thus

$$\frac{\partial e_a}{\partial f} = e_s(T). \tag{13.20}$$

We finally get

$$\frac{\partial ETo}{\partial f} = \frac{\partial ETo_{Rad}}{\partial R_{nl}}\frac{\partial R_{nl}}{\partial e_a}\frac{\partial e_a}{\partial f} + \frac{\partial ETo_{Vent}}{\partial e_a}\frac{\partial e_a}{\partial f} \tag{13.21}$$

with $\left[\frac{\partial ETo}{\partial f}\right] = \frac{mm}{day\%}$.

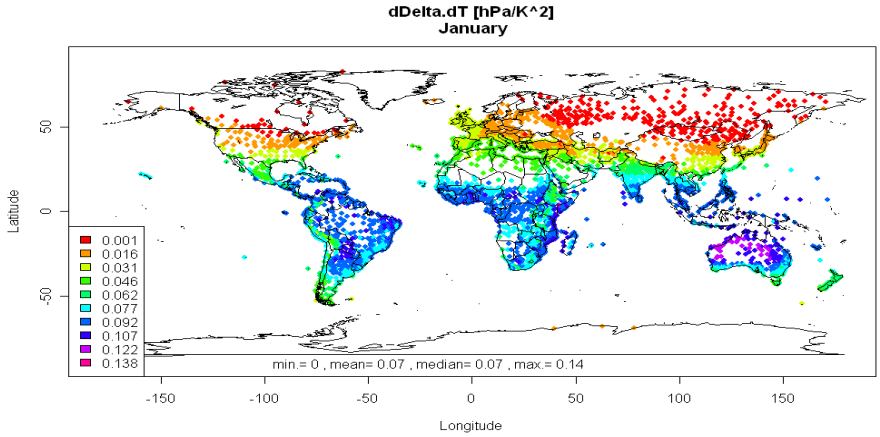

Figure 13.1: $\frac{d\Delta}{dT}\left[\frac{hPa}{K^2}\right]$, *January.*

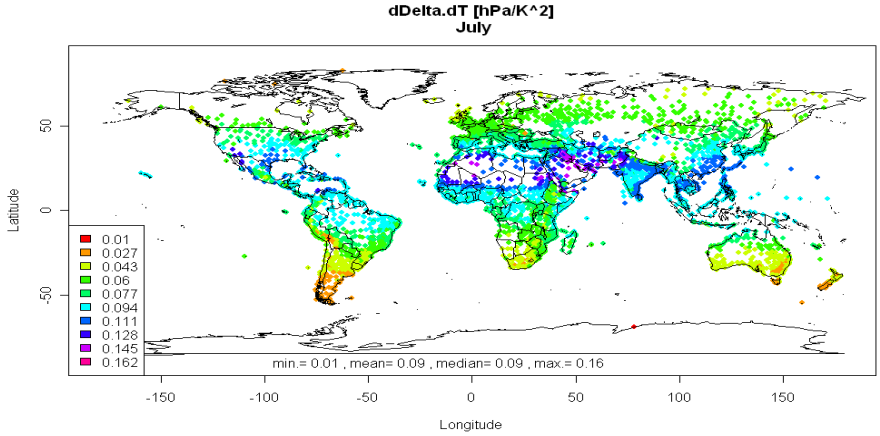

Figure 13.2: $\frac{d\Delta}{dT}\left[\frac{hPa}{K^2}\right]$, *July.*

13.3 Radiation

13.3.1 Net Radiation

The derivative of ETo with net radiation is simply

$$\frac{\partial ETo}{\partial R_n} = \frac{\Delta}{L(\Delta+\gamma)(1+0.34u_2)} \tag{13.22}$$

and since $R_n = R_{ns} - R_{nl}$ we get

$$\frac{\partial ETo}{\partial R_{ns}} = \frac{\partial ETo}{\partial R_n}\frac{\partial R_n}{\partial R_{ns}} = \frac{\Delta}{L(\Delta+\gamma)(1+0.34u_2)} \tag{13.23}$$

and

$$\frac{\partial ETo}{\partial R_{nl}} = \frac{\partial ETo}{\partial R_n}\frac{\partial R_n}{\partial R_{nl}} = -\frac{\Delta}{L(\Delta+\gamma)(1+0.34u_2)} \tag{13.24}$$

We see that the sensitivity of ETo with both, longwave and shortwave radiation balance, becomes smaller with increasing wind speed and increasing temperatures (since Δ and γ are monotonic functions of T).

13.3.2 Shortwave Radiation

According to equation (8.9) it is obvious that the sensitivity of net shortwave radiation R_{ns} with respect to downwelling shortwave radiation at the surface R_s is

$$\frac{\partial R_{ns}}{\partial R_s} = (1 - \alpha) \tag{13.25}$$

which is 0.77 in case of reference grass. Furthermore, according to eq. (8.6) we get

$$\frac{\partial R_s}{\partial R_a} = a_s + b_s \frac{n}{N} \tag{13.26}$$

and

$$\frac{\partial R_s}{\partial \left(\frac{n}{N}\right)} = b_s R_a. \tag{13.27}$$

13.3.3 Longwave Radiation

According to eq. (8.10) the longwave radiation balance is

$$R_{nl} = \sigma \frac{T_n^4 + T_x^4}{2} \times C_v \times C_c \tag{13.28}$$

with

$$C_v = 0.34 - 0.14\sqrt{e_a/10hPa} \tag{13.29}$$

and

$$C_c = 1.35 \frac{R_s}{R_{s0}} - .35 \tag{13.30}$$

The longwave radiation balance is determined by T_x, T_n, e_a, and $\frac{R_s}{R_{s0}}$. The latter is a function of the sunshine fraction $\frac{n}{N}$ as

$$\frac{R_s}{R_{s0}} = \frac{(a_s + b_s \frac{n}{N})}{a_s + b_s + 2 \cdot 10^{-5} z} = A + B \frac{n}{N} \tag{13.31}$$

with $A = \frac{a_s}{a_s + b_s 2 \cdot 10^{-5} z}$ and

$$B = \frac{b_s}{a_s + b_s + 2 \cdot 10^{-5} z} = \frac{\partial (R_s/R_{s0})}{\partial (n/N)}. \tag{13.32}$$

Furthermore we get

$$\frac{\partial C_v}{\partial e_a} = -\frac{0.14}{20hPa\,\sqrt{e_a/10hPa}} \tag{13.33}$$

and

$$\frac{\partial C_c}{\partial \frac{n}{N}} = \frac{\partial C_c}{\partial \frac{R_s}{R_{s0}}} \frac{\partial \frac{R_s}{R_{s0}}}{\partial \frac{n}{N}} = 1.35\, B \tag{13.34}$$

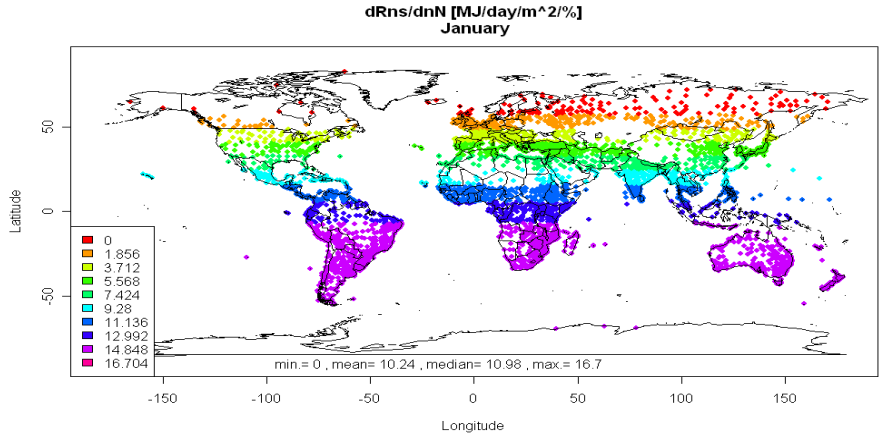

Figure 13.3: Derivative of net shortwave radiation at the surface with sunshine fraction $\frac{\partial R_{ns}}{\partial nN}\left[\frac{MJ/day/m^2}{\%}\right]$*, January.*

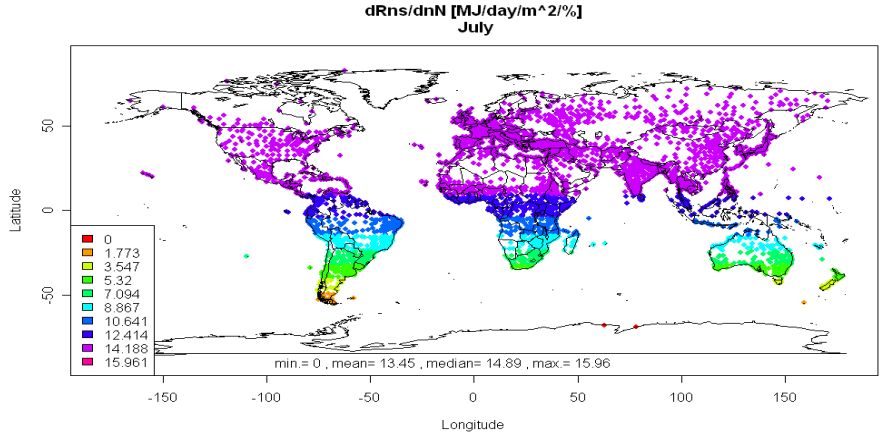

Figure 13.4: Derivative of net shortwave radiation at the surface with sunshine fraction $\frac{\partial R_{ns}}{\partial nN}\left[\frac{MJ/day/m^2}{\%}\right]$*, July.*

For the partial derivatives we get directly

$$\begin{aligned}
\frac{\partial R_{nl}}{\partial (n/N)} &= \frac{\partial R_{nl}}{\partial C_c}\frac{\partial C_c}{\partial \frac{R_s}{R_{s0}}}\frac{\partial \frac{R_s}{R_{s0}}}{\partial \frac{n}{N}} = \sigma\frac{T_n^4+T_x^4}{2}C_v\,1.35\,B \\
\frac{\partial R_{nl}}{\partial e_a} &= \frac{\partial R_{nl}}{\partial C_v}\frac{\partial C_v}{\partial e_a}\frac{\partial e_a}{\partial f} = -\sigma\frac{T_n^4+T_x^4}{2}C_c\,0.14\cdot 0.5(e_a/10hPa)^{-0.5} \\
\frac{\partial R_{nl}}{\partial T_k} &= \sigma C_v C_c 2T_k^3
\end{aligned} \tag{13.35}$$

where T_k stands for T_x and T_n, since the structure of the sensitivity of the longwave radiation balance on maximum and minimum temperature is the same.

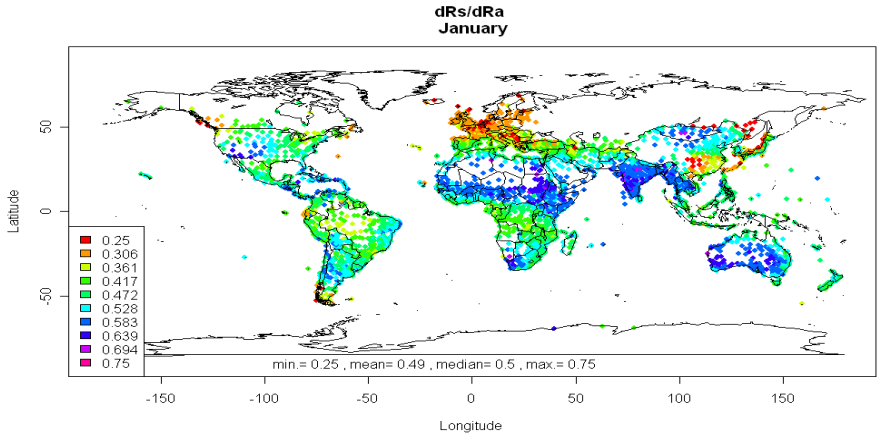

Figure 13.5: Deviation of the surface incoming solar radiation with the extraterrestrial solar radiation $\frac{\partial R_s}{\partial R_a}$ January.

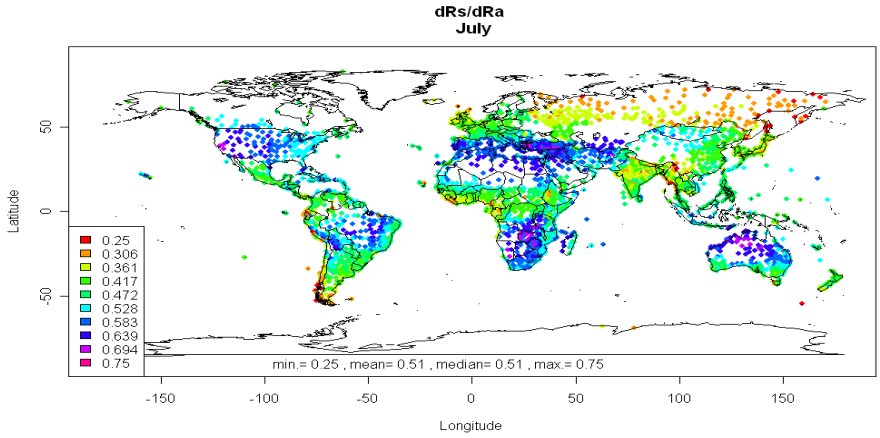

Figure 13.6: Deviation of the surface incoming solar radiation with the extraterrestrial solar radiation $\frac{\partial R_s}{\partial R_a}$, July.

13.4 Wind Speed

ETo can be written as a function of u_2 in the form

$$ETo = \frac{k}{l + mu_2} + \frac{r\,u_2}{l + mu_2} = y_1 + y_2 \tag{13.36}$$

with

$$\begin{aligned} k &= \frac{\Delta}{L}(R_n - G) \\ l &= \Delta + \gamma \\ m &= 0.34\,\gamma \\ r &= \gamma\frac{90}{T}(e_s - e_a). \end{aligned} \tag{13.37}$$

After short calculus we see

$$\begin{aligned} \frac{dy_1}{du_2} &= \frac{-k\,m}{(l+mu_2)^2} \\ \frac{dy_2}{du_2} &= \frac{r\,l}{(l+mu_2)^2} \end{aligned} \tag{13.38}$$

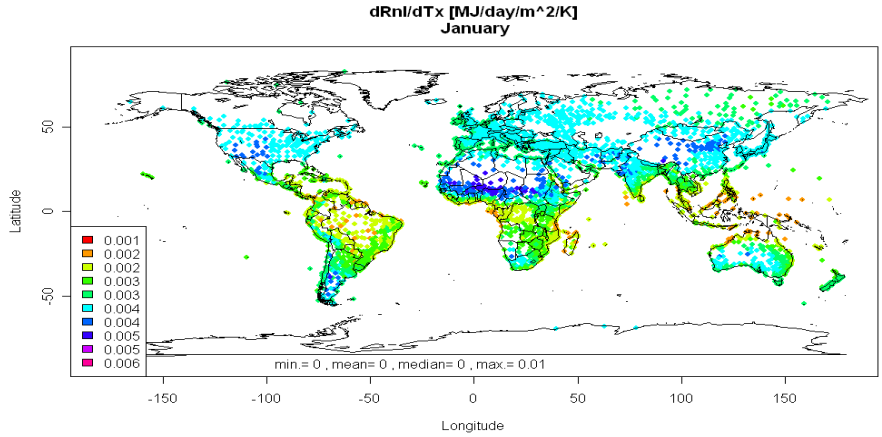

Figure 13.7: Derivative of the net longwave radiation at the surface with mean daily maximum temperature $\frac{\partial R_{nl}}{\partial T_x}\left[\frac{MJ}{m^2 day\, K}\right]$*, January.*

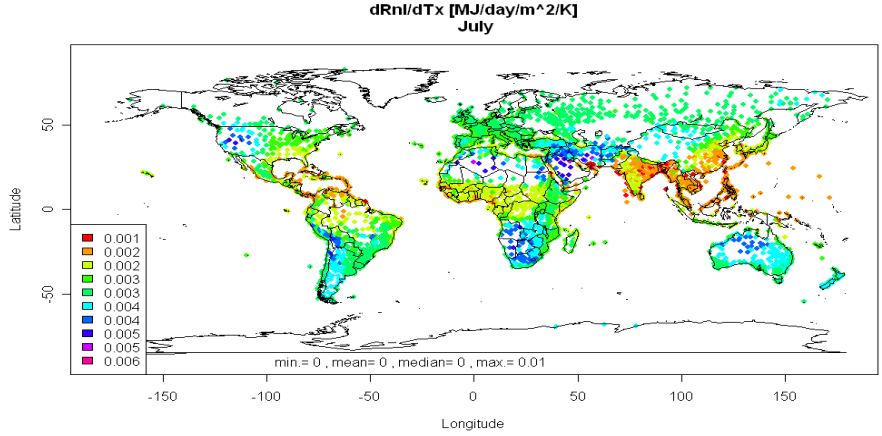

Figure 13.8: Derivative of the net longwave radiation at the surface with mean daily maximum temperature $\frac{\partial R_{nl}}{\partial T_x}\left[\frac{MJ}{m^2 day\, K}\right]$*, July.*

and thus

$$\frac{dETo}{du_2} = \frac{r\,l - k\,m}{(l + mu_2)^2}. \tag{13.39}$$

13.5 Relative Sensitivities

We can divide the sensitivities by ETo itself in order to get relative sensitivities expressed in % change per change of an independent variable x

$$\frac{100}{ETo}\frac{\partial ETo}{\partial x}. \tag{13.40}$$

Results for one station are shown in section 13.7.

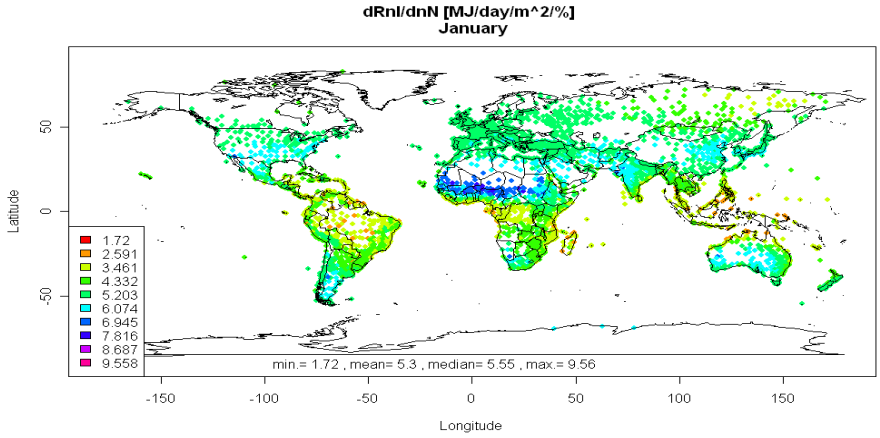

Figure 13.9: Derivative of the net longwave radiation at the surface with sunshine fraction $\frac{\partial R_{nl}}{\partial nN}\left[\frac{MJ}{m^2 day\,\%}\right]$*, January.*

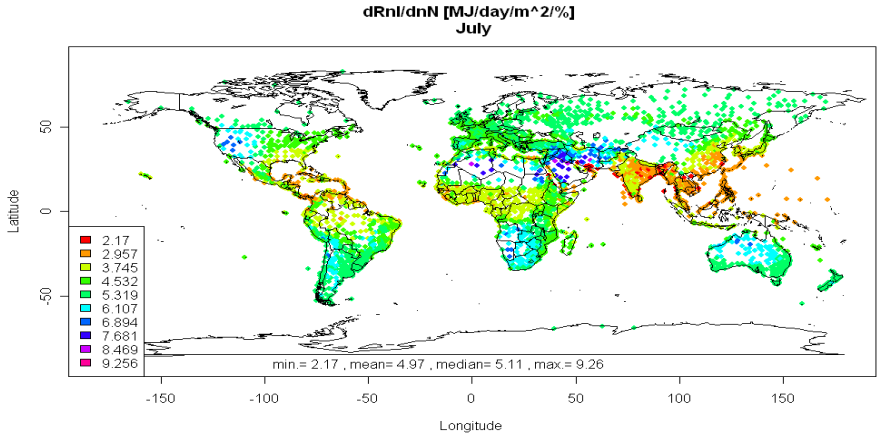

Figure 13.10: Derivative of the net longwave radiation at the surface with sunshine fraction $\frac{\partial R_{nl}}{\partial nN}\left[\frac{MJ}{m^2 day\,\%}\right]$*, July.*

13.6 Ratios of Sensitivities

We now ask how much one variable x must change in order to compensate for changes in another variable y. Given the known sensitivities we look for

$$\frac{\partial ETo}{\partial x}\delta x = -\frac{\partial ETo}{\partial y}\delta y \tag{13.41}$$

and thus

$$\frac{\delta x}{\delta y} = \frac{-\frac{\partial ETo}{\partial y}}{\frac{\partial ETo}{\partial x}}. \tag{13.42}$$

These ratios can be calculated for each pair of variables. Here, we concentrate on the question how much a variable x must change in order to compensate changes in a symmetric temperature increase $y = T$ with $dT = dT_n = dT_x$.

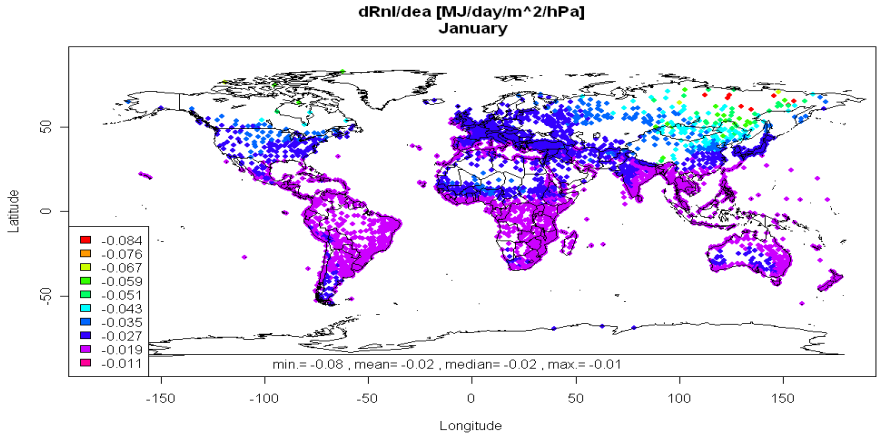

Figure 13.11: Derivative of the net longwave radiation at the surface with water vapor pressure $\frac{\partial R_{nl}}{\partial de_a}\left[\frac{MJ}{m^2 day\, hPa}\right]$*, January.*

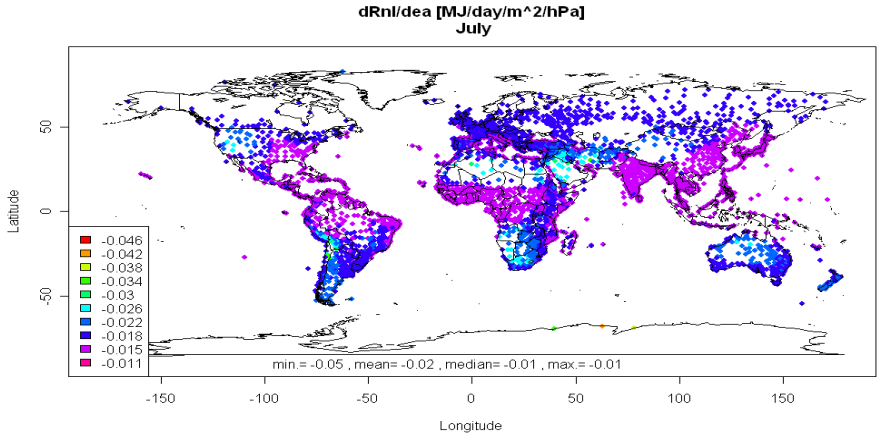

Figure 13.12: Derivative of the net longwave radiation at the surface with water vapor pressure $\frac{\partial R_{nl}}{\partial de_a}\left[\frac{MJ}{m^2 day\, hPa}\right]$*, July.*

13.7 Results for Bangkok

Example: Bangkok (April)

13.7.1 Basic Derivatives

$$
\begin{array}{rcl|rcl}
\frac{d\Delta}{dT} & = & 0.1223972\frac{hPa}{K^2} & \frac{dRns}{dnN} & = & 0.14652\frac{MJ}{m^2\, day\, \%} \\
\frac{d\Delta}{dT_n} & = & 0.0611986\frac{hPa}{K^2} & \frac{dRnl}{dnN} & = & 0.038783\frac{MJ}{m^2\, day\, \%} \\
\frac{d\Delta}{dT_x} & = & 0.0611986\frac{hPa}{K^2} & \frac{dRnl}{de_a} & = & -0.1243379\frac{MJ}{m^2\, day\, hPa} \\
\frac{dRns}{dRs} & = & 0.77 & \frac{dRnl}{df} & = & -0.05497398\frac{MJ}{m^2\, day\, \%} \\
\frac{dRs}{dRa} & = & 0.5951756 & \frac{de_a}{df} & = & 0.4421338\frac{hPa}{\%} \\
\frac{dRs}{dnN} & = & .19029\frac{MJ}{m^2\, day\, \%} & \frac{dR_{nl}}{dT_x} & = & 0.02140941\frac{MJ}{m^2\, day\, K} \\
\frac{dRns}{dRa} & = & 0.4582852 & \frac{dR_{nl}}{dT_x} & = & 0.01954735\frac{MJ}{m^2\, day\, K}
\end{array}
$$

$$
\begin{array}{rcl|rcl}
\frac{dETo_{vent}}{de_a} & = & -0.1113343\frac{mm}{day\,hPa} & \frac{dETo_{rad}}{du_2} & = & -0.2529699\frac{mm\,s}{day\,m} \\
\frac{dETo_{rad}}{de_a} & = & 0.03473894\frac{mm}{day\,hPa} & \frac{dETo_{vent}}{du_2} & = & 0.7631152\frac{mm\,s}{day\,m} \\
\frac{dETo}{de_a} & = & -0.07659532\frac{mm}{day\,hPa} & \frac{dETo}{du_2} & = & 0.5101453\frac{mm\,s}{day\,m} \\
\frac{dETo}{dR_{nl}} & = & -0.2793915\frac{mm\,day\,m^2}{day\,MJ} & \frac{dETo_{rad}}{dT_n} & = & 0.02565998\frac{mm}{day\,K} \\
\frac{dETo}{dR_n s} & = & 0.2793915\frac{mm\,day\,m^2}{day\,MJ} & \frac{dETo_{rad}}{dT_x} & = & 0.02513692\frac{mm}{day\,K} \\
\frac{dETo}{dR_n} & = & 0.2793915\frac{mm\,day\,m^2}{day\,MJ} & \frac{dETo_{vent}}{dT_n} & = & 0.07563974\frac{mm}{day\,K} \\
\frac{dETo_{rad}}{df} & = & 0.01535926\frac{mm}{day\,\%} & \frac{dETo_{vent}}{dT_x} & = & 0.1386271\frac{mm}{day\,K} \\
\frac{dETo_{vent}}{df} & = & -0.04922464\frac{mm}{day\,\%} & \frac{dETo}{dT_x} & = & 0.1637668\frac{mm}{day\,K} \\
\frac{dETo}{df} & = & -0.03386538\frac{mm}{day\,\%} & \frac{dETo}{dT_n} & = & 0.1012997\frac{mm}{day\,K} \\
\frac{dETo}{dR_a} & = & 0.1280410\frac{mm\,day\,m^2}{day\,MJ} & \frac{dETo}{dT_{sym}} & = & 0.2650666\frac{mm}{day\,K} \\
\frac{dETo}{dnN} & = & .030101\frac{mm}{day\,\%} & & &
\end{array}
$$

13.7.2 Relative Sensitivities

$$
\begin{array}{rcl|rcl}
\frac{1}{ETo}\frac{dETo_{vent}}{de_a} & = & -1.95\frac{\%}{hPa} & \frac{1}{ETo}\frac{dETo_{rad}}{du_2} & = & -4.43\frac{\%\,s}{m} \\
\frac{1}{ETo}\frac{dETo_{rad}}{de_a} & = & 0.61\frac{\%}{hPa} & \frac{1}{ETo}\frac{dETo_{vent}}{du_2} & = & 13.35\frac{\%\,s}{m} \\
\frac{1}{ETo}\frac{dETo}{de_a} & = & -1.34\frac{\%}{hPa} & \frac{1}{ETo}\frac{dETo}{du_2} & = & 8.93\frac{\%\,s}{m} \\
\frac{1}{ETo}\frac{dETo}{dR_{nl}} & = & -4.89\frac{\%\,day\,m^2}{MJ} & \frac{1}{ETo}\frac{dETo_{rad}}{dT_n} & = & 0.449\frac{\%}{K} \\
\frac{1}{ETo}\frac{dETo}{dR_n s} & = & 4.89\frac{\%\,day\,m^2}{MJ} & \frac{1}{ETo}\frac{dETo_{rad}}{dT_x} & = & 0.439\frac{\%}{K} \\
\frac{1}{ETo}\frac{dETo}{dR_n} & = & 4.89\frac{\%\,day\,m^2}{MJ} & \frac{1}{ETo}\frac{dETo_{vent}}{dT_n} & = & 1.323\frac{\%}{K} \\
\frac{1}{ETo}\frac{dETo_{rad}}{df} & = & 0.27\frac{\%}{\%} & \frac{1}{ETo}\frac{dETo_{vent}}{dT_x} & = & 2.425\frac{\%}{K} \\
\frac{1}{ETo}\frac{dETo_{vent}}{df} & = & -0.86\frac{\%}{\%} & \frac{1}{ETo}\frac{dETo}{dT_x} & = & 2.86\frac{\%}{K} \\
\frac{1}{ETo}\frac{dETo}{df} & = & -0.59\frac{\%}{\%} & \frac{1}{ETo}\frac{dETo}{dT_n} & = & 1.772\frac{\%}{K} \\
\frac{1}{ETo}\frac{dETo}{dR_a} & = & 2.24\frac{\%\,day\,m^2}{MJ} & \frac{1}{ETo}\frac{dETo}{dT_{sym}} & = & 4.638\frac{\%}{K} \\
\frac{1}{ETo}\frac{dETo}{dnN} & = & 0.523\frac{\%}{\%} & & &
\end{array}
$$

13.7.3 Ratios of Sensitivities

Here we provide some results of eq. (13.42) for the case of Bangkok in April

$$
\begin{aligned}
-\frac{\frac{dETo}{dT_{sym}}}{\frac{dETo}{du_2}} &= -0.51959\frac{m/s}{K} \\
-\frac{\frac{dETo}{dT_{sym}}}{\frac{dETo}{dR_n}} &= -0.9487282\frac{MJ/m^2/day}{K} \\
-\frac{\frac{dETo}{dT_{sym}}}{\frac{dETo}{de_a}} &= +3.460610\frac{hPa}{K} \\
-\frac{\frac{dETo}{dT_{sym}}}{\frac{dETo}{df}} &= +7.827066\frac{\%}{K} \\
-\frac{\frac{dETo}{dT_{sym}}}{\frac{dETo}{dnN}} &= -8.805762\frac{\%}{K}
\end{aligned}
$$

The results for the global dataset are provided in figures 13.13 to 13.20.

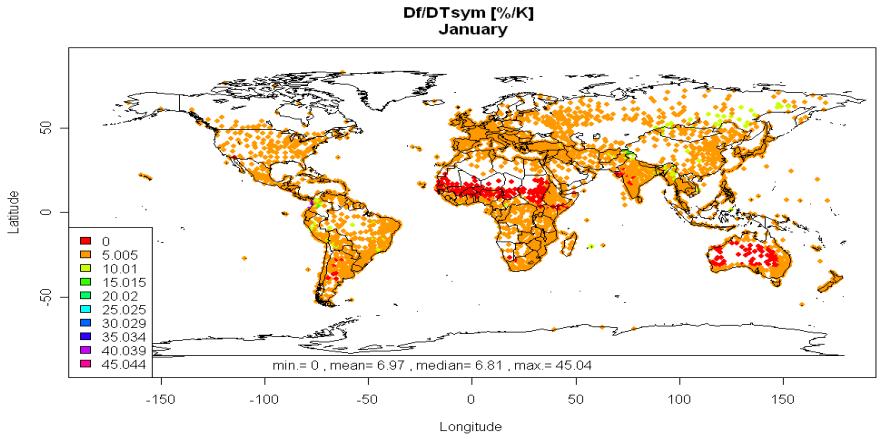

Figure 13.13: Necessary change of rel. humidity $\frac{\Delta f}{\Delta T_{sym}} \left[\frac{\%}{K}\right]$ *in order to compensate a change in temperature which is identical in maximum and minimum temperature, January.*

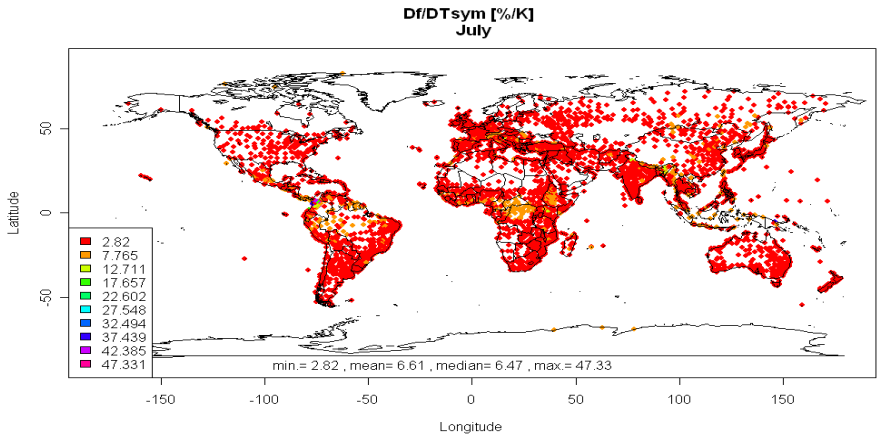

Figure 13.14: Necessary change of rel. humidity $\frac{\Delta f}{\Delta T_{sym}} \left[\frac{\%}{K}\right]$ *in order to compensate a change in temperature which is identical in maximum and minimum temperature, July.*

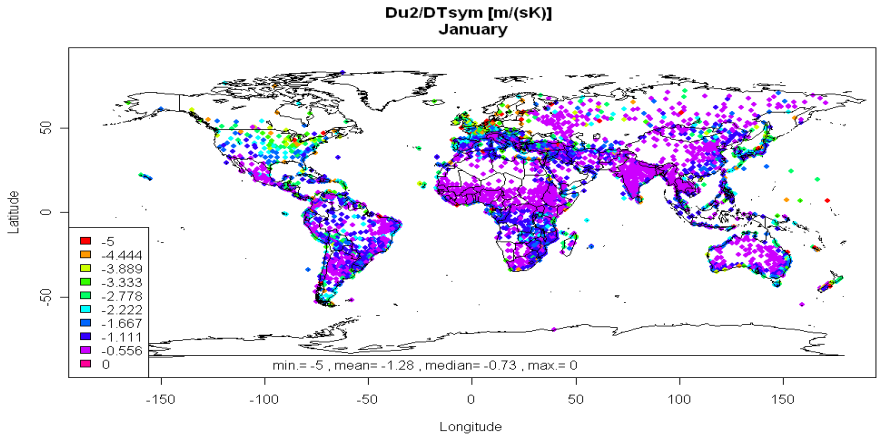

Figure 13.15: Necessary change in wind speed $\frac{\Delta u_2}{\Delta T_{sym}}\left[\frac{m/s}{K}\right]$ *in order to compensate a change in temperature which is identical in maximum and minimum temperature, January.*

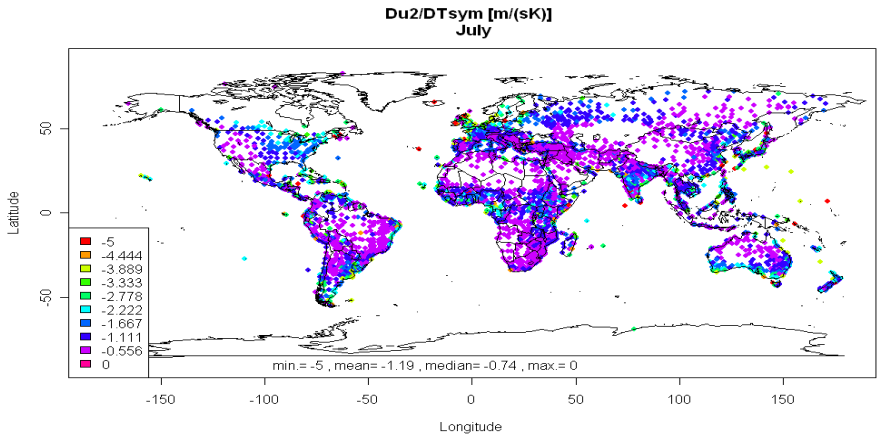

Figure 13.16: Necessary change in wind speed $\frac{\Delta u_2}{\Delta T_{sym}}\left[\frac{m/s}{K}\right]$ *in order to compensate a change in temperature which is identical in maximum and minimum temperature, July.*

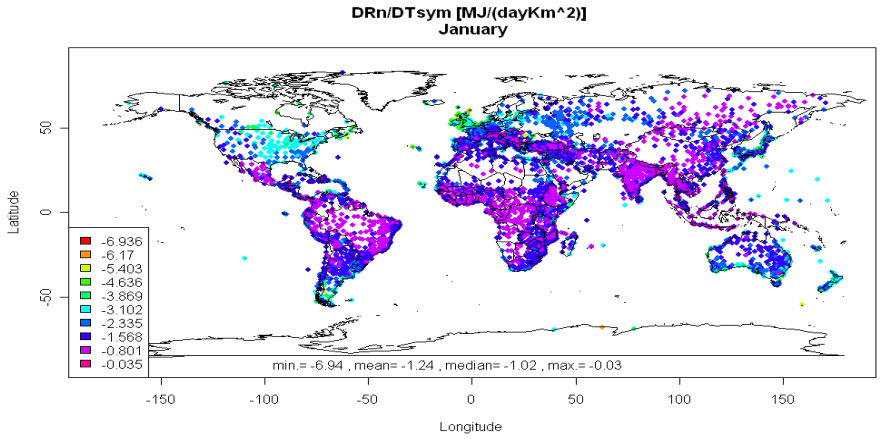

Figure 13.17: Necessary change in surface net radiation balance $\frac{\Delta R_n}{\Delta T_{sym}}$ $\left[\frac{MJ/day/m^2}{K}\right]$ *in order to compensate a change in temperature which is identical in maximum and minimum temperature, January.*

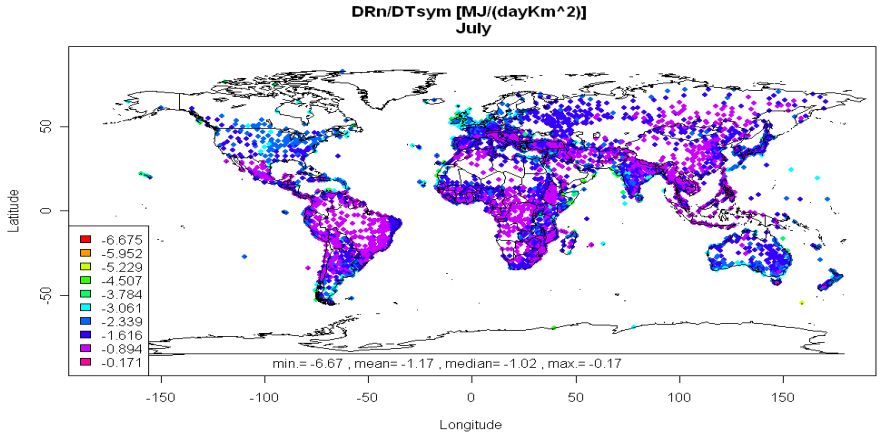

Figure 13.18: Necessary change in surface net radiation balance $\frac{\Delta R_n}{\Delta T_{sym}}$ $\left[\frac{MJ/day/m^2}{K}\right]$ *in order to compensate a change in temperature which is identical in maximum and minimum temperature, July.*

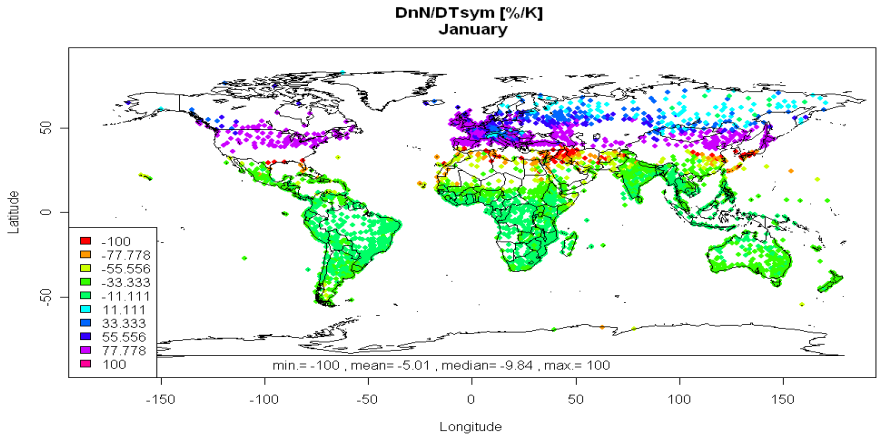

Figure 13.19: Necessary change in sunshine fraction $\frac{\Delta nN}{\Delta T_{sym}}$ $\left[\frac{\%}{K}\right]$ *in order to compensate a change in temperature which is identical in maximum and minimum temperature, January.*

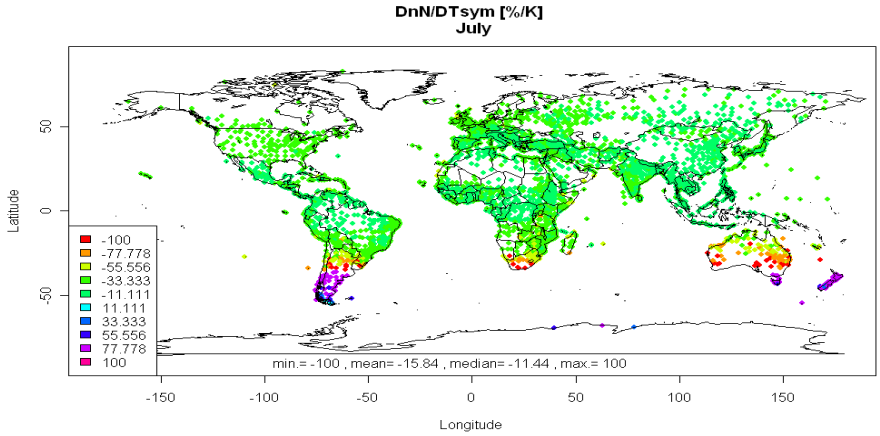

Figure 13.20: Necessary change in sunshine fraction $\frac{\Delta nN}{\Delta T_{sym}}$ $\left[\frac{\%}{K}\right]$ *in order to compensate a change in temperature which is identical in maximum and minimum temperature, July.*

Appendix A

Latent Heat of Evaporation as Function of Temperature

According to Rogers and Yau (1989) the latent heat of evaporation L can be written as

$$L = \frac{kJ}{kg}(-0.0000614342\frac{T^3}{^\circ C^3} + 0.00158927\frac{T^2}{^\circ C^2} - 2.36418\frac{T}{^\circ C} + 2500.79) \tag{A.1}$$

with a coefficient of determination of $r^2 = 0.999988$. This relation is depicted in Fig. A.1. It shows clearly that $L = 2.45MJ/kg$ is a good approximation for temperatures about $20°C$. However, for $T = 40°C$ L reduces to about $2.4MJ/kg$ while it is $2.5MJ/kg$ at freezing point and $2.55MJ/kg$ at $-20°C$, resulting in relative differences of up to $0.15/2.45 \approx 6\%$.

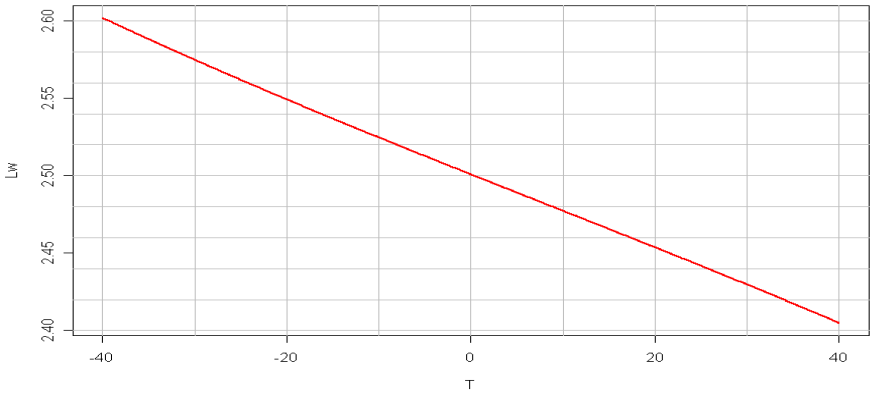

Figure A.1: Temperature dependence of latent heat of evaporation L.

Appendix B

Derivative of Δ

$$\Delta(T) = a \exp\left(\frac{b(T-c)}{T-d}\right) \cdot \frac{1}{(T-d)^2} = u \cdot v \tag{B.1}$$

with

$$\begin{aligned} u &= a \exp\left(\tfrac{b(T-c)}{T-d}\right) \\ u' &= u \tfrac{d}{dt}\left(b(T-c)(T-d^{-1})\right) \\ &= ub\left[-(T-c)(T-d)^{-2} + (T-d)^{-1}\right] \\ &= u\tfrac{b(c-d)}{(T-d)^{-2}} \\ &= b(c-d)\Delta \\ v &= (T-d)^{-2} \\ v' &= -2(T-d)^{-3} \end{aligned} \tag{B.2}$$

and thus

$$\begin{aligned} \tfrac{d\Delta}{dT} &= uv' + vu' \\ &= -2a \exp\left(\tfrac{b(T-c)}{T-d}\right)(T-d)^{-3} + b(c-d)\Delta(T-d)^{-2} \\ &= \tfrac{b(c-d)\Delta}{(T-d)^2} \\ &= \tfrac{\Delta}{T-d}\left\{\tfrac{b(c-d)}{T-d} - 2\right\} \end{aligned} \tag{B.3}$$

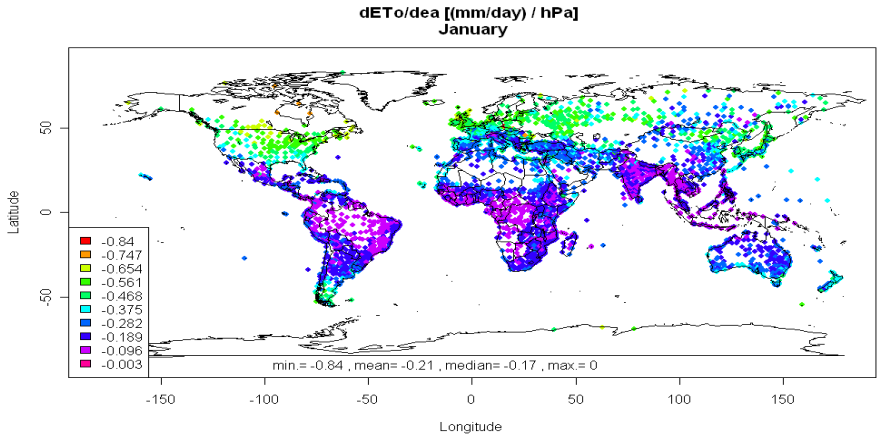

Figure B.1: $\frac{dETo}{de_a}\ \left[\frac{MJ}{m^2\,day\,hPa}\right]$, *January.*

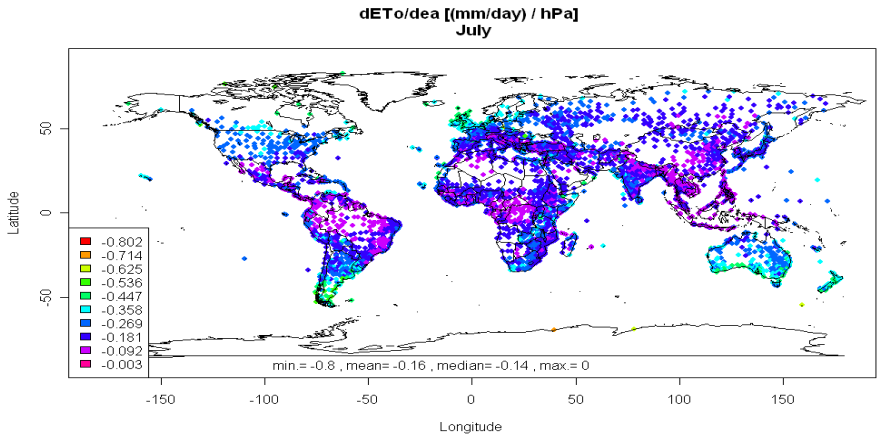

Figure B.2: $\frac{dETo}{de_a}\ \left[\frac{MJ}{m^2\,day\,hPa}\right]$, *July.*

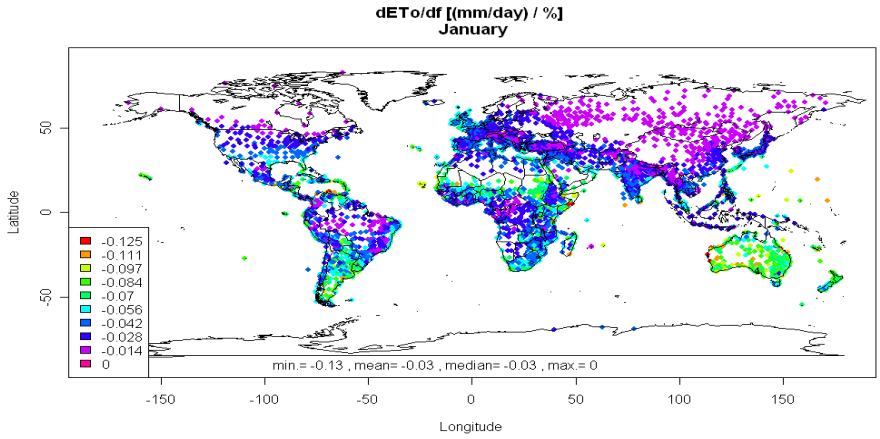

Figure B.3: $\frac{dETo}{df}\ \left[\frac{MJ}{m^2\,day\,\%}\right]$, *January.*

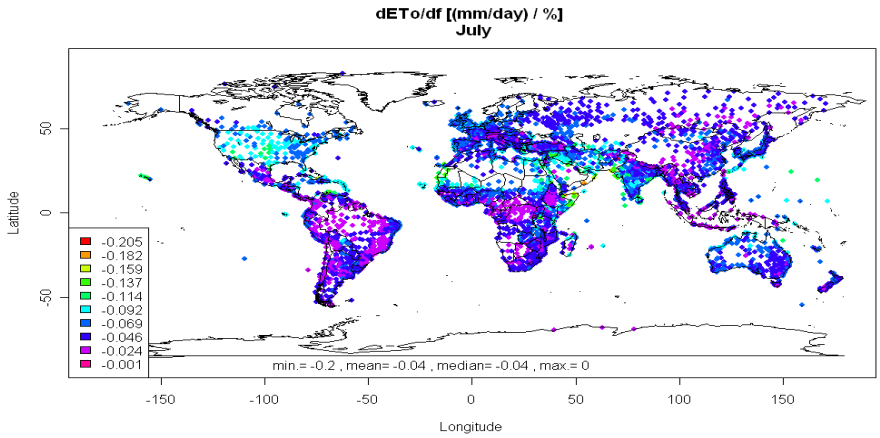

Figure B.4: $\frac{dETo}{df}\ \left[\frac{MJ}{m^2\,day\,\%}\right]$, *July.*

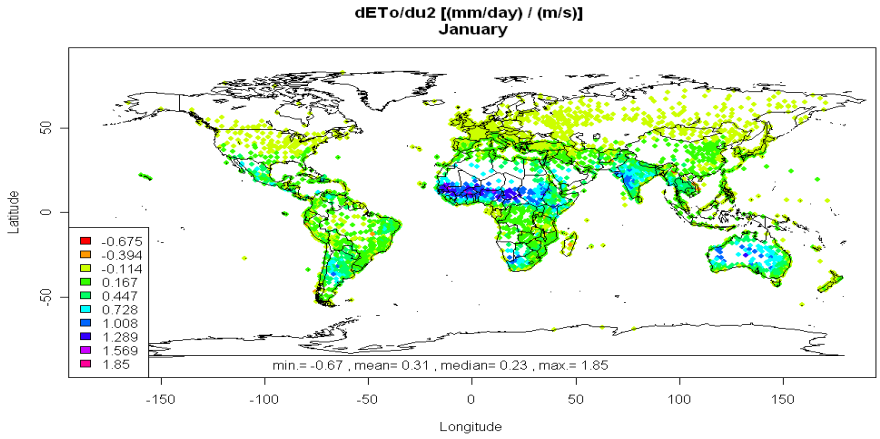

Figure B.5: $\frac{dETo}{du_2}\ \left[\frac{MJ}{m^2\,day\,m/s}\right]$, *January.*

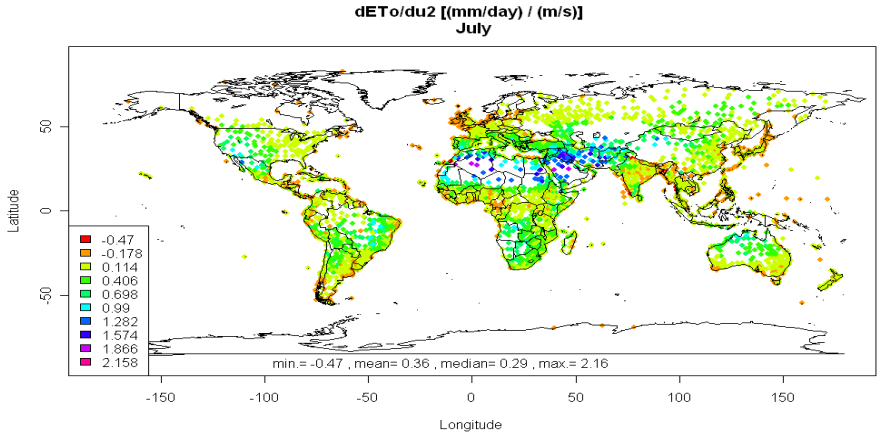

Figure B.6: $\frac{dETo}{du_2}\ \left[\frac{MJ}{m^2\,day\,m/s}\right]$, *July.*

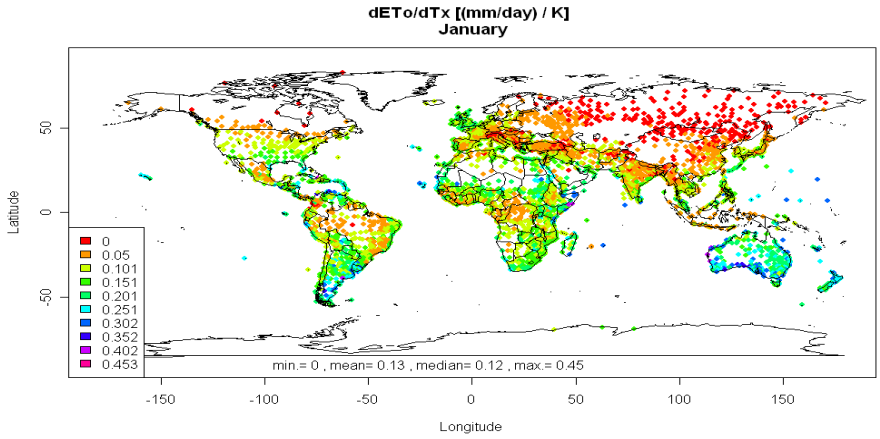

Figure B.7: $\frac{dETo}{dT_x}\left[\frac{MJ}{m^2\,day\,K}\right]$, *January.*

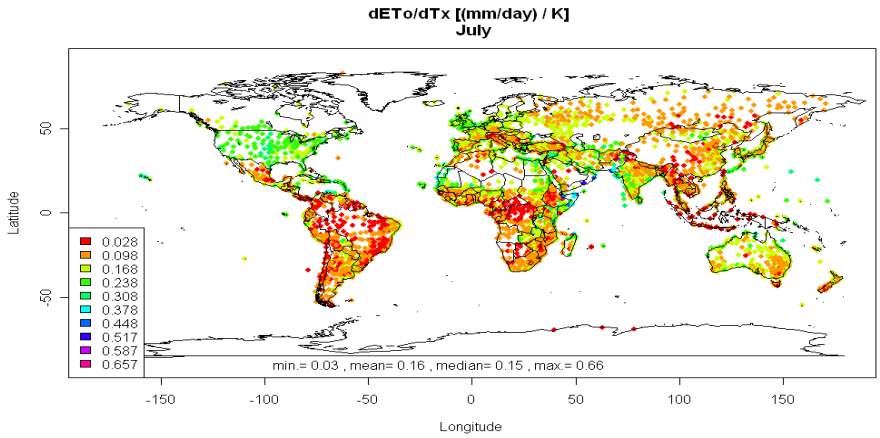

Figure B.8: $\frac{dETo}{dT_x}\left[\frac{MJ}{m^2\,day\,K}\right]$, *July.*

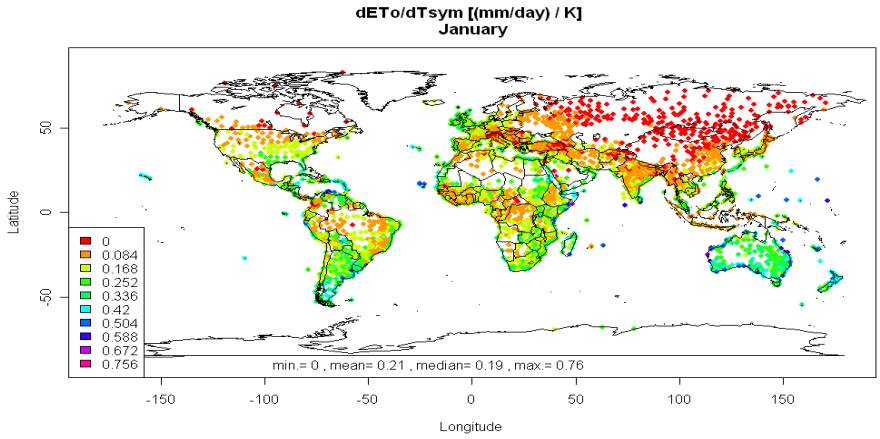

Figure B.9: $\frac{dETo}{dT_{sym}}\ \left[\frac{MJ}{m^2\,day\,K}\right]$, *January.*

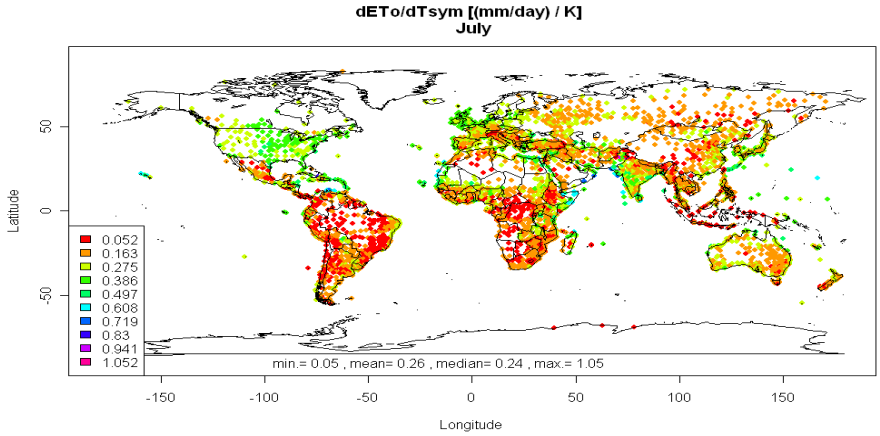

Figure B.10: $\frac{dETo}{dT_{sym}}\ \left[\frac{MJ}{m^2\,day\,K}\right]$, *July.*

Appendix C

Surface Albedo for Solar Radiation

Different surfaces have different reflectivity or albedo α of solar radiation. Table C.1 lists some surfaces with their typical range of surface albedo and a typical value.

Table C.1: Surface albedo of different surfaces in % after Hartmann (1994).

Surface	Range	Typical Value
Water		
Low wind	5 - 10	7
High wind	10 - 20	12
Bare Surfaces		
Moist dark soil	5 - 15	10
Moist grey soil	10 - 20	15
Dry soil	20 - 35	30
Wet sand	20 - 30	25
Dry light sand	30 - 40	35
Asphalt pavement	5 - 10	7
Concrete pavement	15 - 35	20
Vegetation		
FAO reference grass		27
Short green vegetation	10 - 20	17
Dry vegetation	20 - 30	25
Coniferous forest	10 - 15	12
Deciduous forest	15 - 25	17
Snow and Ice		
Forest with snow cover	20 - 35	25
Sea ice	25 - 40	30
Glacier ice	20 - 45	32
Old melting snow	35 - 65	50
Dry cold snow	60 - 75	70
Fresh dry snow	70 - 90	80

Appendix D

Inverse Relative Earth Sun Distance

FAO56 uses eq. (8.3) with J as julian day for the inverse relative earth sun distance.

$$d_r = 1 + 0.033 \cos \frac{2\pi\, J}{365} \tag{D.1}$$

with J as Julian day for the inverse relative earth sun distance. There are, however, other and more accurate approximations available. One example is

$$d_{r2} = \frac{1}{\left[1 - 0.01673 \cdot \cos\left(0.017214 \cdot (J-1)\right)\right]^2}. \tag{D.2}$$

Fig. **??** shows both approximations as well as the relative deviation in % of eq. (D.2) from eq. (D.2). Relative deviations are less than 0.3% and depend strongly on season.

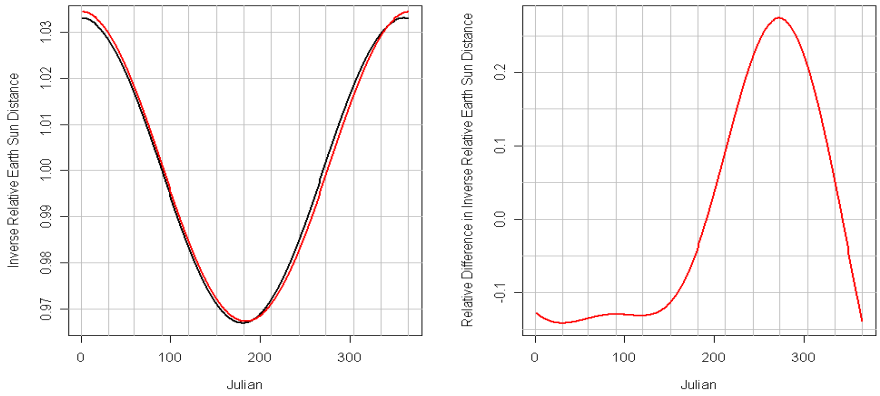

Figure D.1: Inverse relative earth-sun distance as function of Julian day for the approximation used by FAO and a slightly better approximation according to eq. D.2 as well as the relative deviation of the first from the second

Appendix E

Declination

According to eq. 8.2the declination δ as function of the Julian day is approximated as

$$\delta = 0.409 \sin\left(\frac{2\pi\, J}{365} - 1.39\right). \tag{E.1}$$

One better approximation is

$$\delta = \delta_0 + \sum_l imits_i = 1^4 \left(A_i \cos(p_i) + B_i \sin(p_i)\right) \tag{E.2}$$

with

$$p_i = i \cdot p_0 \text{ and } p_0 = .017214 \cdot J - 3.1588 \tag{E.3}$$

and the coefficients $\delta_0 = 0.39508$ and

$$\begin{array}{lllllll} A_1 & = & 22.85684 & B_1 & = & -4.29692 \\ A_2 & = & -0.38637 & B_2 & = & 0.05702 \\ A_3 & = & 0.15097 & B_3 & = & -0.09029 \\ A_4 & = & -0.00961 & B_4 & = & 0.00593 \end{array}$$